

Jan Kvasil; R. G. Nazmitdinov

Semimicroscopical description of the collective states in rotating nuclei - II.

*Acta Universitatis Carolinae. Mathematica et Physica*, Vol. 30 (1989), No. 1, 55--89

Persistent URL: <http://dml.cz/dmlcz/142606>

**Terms of use:**

© Univerzita Karlova v Praze, 1989

Institute of Mathematics of the Academy of Sciences of the Czech Republic provides access to digitized documents strictly for personal use. Each copy of any part of this document must contain these *Terms of use*.



This paper has been digitized, optimized for electronic delivery and stamped with digital signature within the project *DML-CZ: The Czech Digital Mathematics Library* <http://project.dml.cz>

## Semimicroscopical Description of the Collective States in Rotating Nuclei-II

JAN KVASIL

Department of Nuclear Physics, Faculty of Mathematics and Physics, Charles University, Prague\*)

R. G. NAZMITDINOV

Dubna, USSR\*\*)

*Received 30 October 1988*

The method combining the cranking model with the random phase approximation (RPA) is applied for calculation of concrete characteristics of states of rotating nuclei. In broad range of rotational frequencies such a properties of nucleus as energy spectrum, transition probabilities, strength functions, angular momentum alignment are analysed for a number of nuclei. This paper represents a continuation of ref. [1] where the basic ideas of cranking + RPA method were presented.

V práci je aplikována metoda kombinující cranking model (model vynucené rotace) s aproxiací náhodné fáze (Random Phase Approximation RPA) pro výpočet konkrétních charakteristik stavů rotujících jader. V široké oblasti rotačních frekvencí jsou analyzovány energetická spektra, pravděpodobnosti přechodů, precesní pohyb jádra, silové funkce el. mag. přechodů a další vlastnosti pro řadu jader. Práce navazuje na výsledky práce [1], kde byly uvedeny základní myšlenky používané metody.

Метод комбинирующий модель принудительного вращения и приближение случайных фаз применяется для описания конкретных характеристик состояний вращающихся ядер. В широком диапазоне вращательных энергий для ряда ядер анализируются такие свойства как энергетические спектры, вероятности переходов, силовые функции, выстраивание углового момента и другие. Предлагаемая работа является продолжением раб. [1], где были приведены основные идеи использованного метода.

### 1. Introduction

This paper represents the second part of study of the collective states in rotating nuclei. In the first part which is involved in ref. [1] the theoretical problems with the description of the collective excitations of fast rotating nuclei were discussed. Particularly in [1] the method combining the cranking model (CM) with the random phase

\*) V Holešovičkách 2, 180 00 Praha 8, Czechoslovakia

\*\*) Laboratory of Theoretical Physics, JINR Dubna, SV 101 00, USSR

approximation (RPA) was suggested for this purpose. Our first paper [1] on this theme was devoted to the explanation of basic theoretical ideas of CM + RPA approach such as the symmetries of cranking Hamiltonian, the Hartree-Fock-Bogolubov problem for rotating systems, the solutions of RPA equations of motion, selfconsistency of residual interaction with average nuclear field and others.

In this second part the concrete properties of rotating nuclei are studied in the framework of CM + RPA approach. In chapter 2 of this paper the simplified version of CM + RPA model is used for analysis of isoscalar quadrupole and isovector dipole excitations. Chapter 3 is devoted to realistic microscopical calculations of properties of rotating nuclei in broad range of rotational frequencies (i.e. the low-lying states of  $^{168}\text{Er}$  and  $^{158}\text{Dy}$  in § 3.1, the alignment of intrinsic angular momentum in § 3.2, giant dipole resonance at high spins in § 3.3).

## 2. Analysis of collective excitations of rotating nuclei in the simple model

### 2.1. Cranking Hamiltonian in the simple model

The change of nuclear shape and behaviour of nuclear moment of inertia in dependence on rotational frequency  $\Omega$  can be studied within the simple model based on Hamiltonian of harmonic oscillator with effective quadrupole forces [2, 3]. This Hamiltonian contains the average deformed nuclear field and residual quadrupole-quadrupole interaction which is responsible for collective excitations of positive parity [4, 5]. The description of collective excitations with negative parity requires to add the negative parity residual interaction  $H_{RES}^{(-)}$  into the Hamiltonian. So the starting cranking Hamiltonian is

$$(1) \quad H' = \sum_{\nu=1}^A \left( \frac{p_{\nu}^2}{2m} + \frac{m\omega_0^2 r_{\nu}^2}{2} \right) - \frac{\kappa}{2} \sum_{i,k=x,y,z} \hat{Q}_{ik}^2 + H_{RES}^{(-)} - \Omega \hat{L}_x$$

where

$$\hat{Q}_{ik} = \sum_{\nu=1}^A \hat{q}_{ik}(\nu)$$

represent the components of tensor of quadrupole moment of nucleus,

$$\hat{L}_x = \sum_{\nu=1}^A \hat{l}_x(\nu)$$

stands for the operator of angular moment projection onto x-axis and  $\Omega$  is the rotational frequency. Concrete form of  $H_{RES}^{(-)}$  will be given further. In the Hartree approximation the Hamiltonian (1) has the following form

$$(2) \quad H' = H_{S.p.} - \frac{\kappa}{2} \sum_{i=0,1,2} \hat{Q}_i^{(+)^2} - \frac{\kappa}{2} \sum_{i=1,2} \hat{Q}_i^{(-)^2} + H_{RES}^{(-)}$$

where

$$(3) \quad \begin{aligned} \hat{Q}_0^{(+)} &= \sqrt{\frac{3}{2}} (\hat{Q}_{zz} - \langle \Omega | \hat{Q}_{zz} | \Omega \rangle), \quad \hat{Q}_1^{(+)} = \sqrt{2} Q_{yz} \\ \hat{Q}_2^{(+)} &= \sqrt{\frac{1}{2}} (\hat{Q}_{xx} - \langle \Omega | Q_{xx} | \Omega \rangle - \hat{Q}_{yy} + \langle \Omega | \hat{Q}_{yy} | \Omega \rangle) \\ \hat{Q}_1^{(-)} &= \sqrt{2} Q_{xy}, \quad \hat{Q}_2^{(-)} = \sqrt{2} Q_{xz} \end{aligned}$$

where  $\hat{Q}_{ij} = 3\hat{x}_i\hat{x}_j - \delta_{ij}\hat{r}^2$  and  $|\Omega\rangle$  represents the state of yrast line which corresponds to minimal eigen value of single-particle Hamiltonian  $H_{S.p.}$  for given value of rotational frequency  $\Omega$ .

$$(4) \quad \begin{aligned} H_{S.p.}(\Omega) &= \sum_{\nu=1}^A h_{\nu}(\Omega) \\ h_{\nu}(\Omega) &= \frac{P_{\nu}^2}{2m} + \frac{m}{2} (\omega_x^2 x_{\nu}^2 + \omega_y^2 y_{\nu}^2 + \omega_z^2 z_{\nu}^2) - \Omega l_x(\nu) \end{aligned}$$

Following [2] eigen functions and values of single-particle Hamiltonian (4) can be obtained from eq. for creation operator of oscillator quanta  $a_{\lambda}^{\dagger}$  which are defined as a linear combinations of particle coordinate  $\vec{r}$  and linear momentum  $\vec{p}$

$$(6b) \quad \begin{aligned} \begin{pmatrix} x \\ p_x \end{pmatrix} &= \begin{pmatrix} (2m\omega_x)^{-1/2} & (2m\omega_x)^{-1/2} \\ i\left(\frac{m\omega_x}{2}\right)^{1/2} & -i\left(\frac{m\omega_x}{2}\right)^{1/2} \end{pmatrix} \begin{pmatrix} a_x^+ \\ a_x \end{pmatrix} \\ \begin{pmatrix} y \\ z \\ p_y \\ p_z \end{pmatrix} &= \begin{pmatrix} Y_+ & Y_+^* & Y_- & Y_-^* \\ Z_+ & Z_+^* & Z_- & Z_-^* \\ P_+^Y & P_+^{Y*} & P_-^Y & P_-^{Y*} \\ P_+^Z & P_+^{Z*} & P_-^Z & P_-^{Z*} \end{pmatrix} \begin{pmatrix} a_+ \\ a_+^* \\ a_- \\ a_-^* \end{pmatrix} \end{aligned}$$

The explicit form of expressions for transformation coefficients in (6) can be found in [3]. Within the terminology of the operators  $a_{\lambda}^{\dagger}$ ,  $a_{\lambda}$  the Hamiltonian (4) has the following form

$$(7) \quad H_{S.p.} = \sum_{\substack{\nu=1 \\ \sigma=x,+,-}}^A \omega_{\sigma} (\hat{n}_{\sigma} + \frac{1}{2})_{\nu} \equiv \sum_{\sigma} \omega_{\sigma} w_{\sigma}$$

where

$$(8) \quad \begin{aligned} \hat{n}_{\sigma} &= a_{\sigma}^{\dagger}(\nu) a_{\sigma}(\nu) \quad [a_{\sigma}(\nu), a_{\sigma}^{\dagger}(\nu')] = \delta_{\sigma\sigma'} \delta_{\nu\nu'} \\ \omega_{\pm}^2 &= \frac{\omega_y^2 + \omega_z^2}{2} + \Omega \pm \frac{1}{2} [(\omega_y^2 - \omega_z^2)^2 + 8\Omega^2(\omega_y^2 + \omega_z^2)] \end{aligned}$$

The change of shape of rotating nucleus was analysed in detail in [3]. Typical diagram of dependence of equilibrium deformation parameters on rotational frequency is shown in fig. 1. In relatively small angular velocities the value of single-particle potential deformation decreases with increasing  $\Omega$ , but nonaxiality grows up. In angular velocities higher than some critical value  $\Omega_{c2}^{(1)}$  the most profitable shape

shows to be oblate ellipsoid rotating round its symmetry axis. It must be noted that the behaviour of deformation parameters is determined by conditions of energy minimum which in quasi-classical approach can be expressed in the form [3]

$$\omega_x w_x = \omega_+ w_+ = \omega_- w_- = C = \text{const}$$

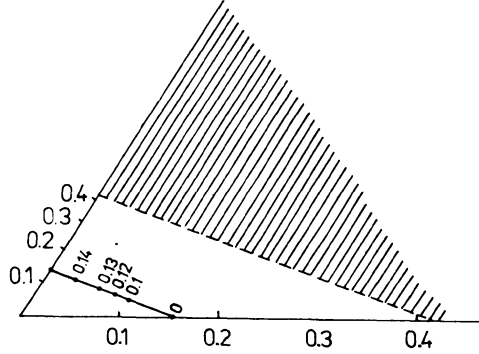


Fig. 1. Dependence of deformation parameters  $\beta$  and  $\gamma$  on rotational frequency  $\Omega$ . Points with numbers determine the corresponding values of  $\Omega/\omega_0$ .

In the absence of rotation these conditions justify consistency of nucleon density with the shape of the oscillator potential [6]. Besides that fixing relations between filling in different rotational axes these conditions give several possibilities corresponding different rotational bands. It is evident that the most favourable from the point of view of energy is the yrast line.

More patent changes in nucleus shape in given model occur in the region of high angular velocities of rotation. In this sense more realistic description of behaviour of deformation seems to be obtained in the framework of the liquid drop model [7]. Similarly to realistic CM + RPA model simple model used in this chapter describes the collective excitations by means of phonon which can be expressed in terms of generalized coordinate and linear momenta (see rel. (30) in [1]). These coordinates and momenta fulfil the RPA equations of motion (28) in [1]. Since the Hamiltonian (2) is invariant with respect to rotation by angle  $\pi$  round the axis  $x$  in accordance with § 2.3.1 in [1] the operators of phonons can be characterised in RPA by quantum number of signature  $\pm$

$$(10) \quad R_x(\pi) O_v^+ R_x^{-1}(\pi) = \pm O_v^+$$

and it is possible to divide the residual interactions in (2) into four mutually commuting parts  $H_{RES}^{(\pm)(\pm)}$  (similarly as in (20) of [1])

$$(11) \quad H' = H_{S.p.} + H_{RES}^{(+)}(+) + H_{RES}^{(-)}(+) + H_{RES}^{(+)}(-) + H_{RES}^{(-)}(-)$$

where

$$(12a) \quad H_{RES}^{(+)}(+)= -\frac{\kappa}{2} \sum_{i=0,1,2} \hat{Q}_i^{(+)^2} \quad H_{RES}^{(-)}(+)= -\frac{\kappa}{2} \sum_{i=1,2} \hat{Q}_i^{(+)^2}$$

$$(12b) \quad H_{RES}^{(-)} = H_{RES}^{(+)}(-) + H_{RES}^{(-)}(-)$$

## 2.2. Isocalar quadrupole excitations

### 2.2.1. Analysis of spectrum

Generalised coordinate and linear momenta for Hamiltonian  $H_{S.p.} = H_{RES}^{(+)}(+) + H_{RES}^{(-)}(+)$  (Hamiltonian of isoscalar forces) can be expressed in the form

$$(13) \quad X_s^{(\pm)} = \sum_s X_s^v(\pm) \hat{q}^{(\pm)}, \quad \mathcal{P}_s^{(\pm)} = i \sum_s \mathcal{P}_s^v(\pm) \hat{p}_s^{(\pm)}$$

where  $\hat{q}_s^{(\pm)}$ ,  $\hat{p}_s^{(\pm)}$  are the bilinear combinations of the operators  $a_\lambda^+$  and  $a_\lambda$ . The concrete form of these combinations is given in [9]. Linearization of equation of motion (Random phase approximation) is obtained by substitution

$$(14) \quad [\hat{q}_s^{(\pm)}, \hat{p}_s^{(\pm)}] \rightarrow [\hat{q}_s^{(\pm)}, \hat{p}_s^{(\pm)}]_{RPA} \equiv \langle \Omega | [\hat{q}_s^{(\pm)}, \hat{p}_s^{(\pm)}] | \Omega \rangle = V_s^{(\pm)} \delta_{ss'}$$

where the quantity  $V_s^{(\pm)}$  represents the  $c$ -number. Following the method of solving of RPA equations of motion for unknowns  $X_s^v(\pm)$  and  $\mathcal{P}_s^v(\pm)$  given in [1] (see § 2.3.2) one can obtain the system of algebraic equations of type (46) and (51) in [1]. The dimension of this system of equation is 3 for positive signature ( $n_1 = 2, n_2 = 1, n_1 + n_2 = 3$  - see [1]) and 2 for negative signature ( $n_1 = n_2 = 1, n_1 + n_2 = 2$ ). The condition of solving of these systems of equations gives us the secular equations for energies  $\omega$  of one-phonon quadrupole states with positive or negative signature for given value of rotational frequency  $\Omega$ . Extraction of spurious modes among the solutions of RPA equations of motion can be performed by the method described in [1].

If the rotation is not present the solution of mentioned above systems of algebraic equations can be classified by the usual way according to projection  $K^\pi$  of angular momentum onto symmetry axis. Spectrum of excitations with positive parity is determined for every value  $K^\pi = 0^+, 1^+, 2^+$  from equation

$$(15) \quad 1 - 2\kappa S_{KK}(\omega) = 0$$

where (see (47) in [1])

$$(16) \quad S_{KK}(\omega) = S(\omega)_{Q_k \pm Q_k^{(\pm)}} = \sum_{\mu\nu} \frac{(\omega_\mu + \omega_\nu) (Q_k^{(\pm)})_{\mu\nu} (Q_k^{(\pm)})_{\mu\nu}}{(\omega_\mu + \omega_\nu)^2 - \omega^2}.$$

Matrix elements  $(Q_k)_{\mu\nu}$  can be obtained in terms of the coefficients of transformation (6) and eventually (15) has the following form

$$\frac{4}{3} \frac{v_x}{4v_z - v} + \frac{2}{3} \frac{v_z}{4v_x - v} = 1 \quad \text{for } K^\pi = 0$$

$$(17) \quad \frac{(v_x - v_z)^2 - v(v_x + v_z)}{(v_x + v_z - v)^2 - 4v_x v_z} = 1 \quad \text{for } K^\pi = 1$$

$$\frac{2v_z}{4v_x - v} = 1 \quad \text{for } K^\pi = 2$$

where  $v \equiv \omega^2/\omega_0^2$ ,  $v_{x,z} = \omega_{x,z}^2/\omega_0^2$ . The solution of these equations is

$$\left. \begin{array}{l} \omega_2(O_{\sigma=+}^+)/\omega_0 \\ \omega_1(O_{\sigma=+}^+)/\omega_0 \end{array} \right\} = [3 - \frac{4}{3}\delta \pm (1 + \frac{8}{3}\delta + \frac{208}{9}\delta^2)^{1/2}]^{1/2} \approx \begin{cases} 2 \\ \sqrt{2}(1 - \frac{2}{3}\delta) \end{cases}$$

$$\omega(1_{\sigma=\pm}^+)/\omega_0 = \sqrt{[2(1 - \frac{1}{3}\delta)]} \approx \sqrt{2}(1 - \frac{1}{6}\delta)$$

$$\omega(2_{\sigma=\pm}^+)/\omega_0 = \sqrt{[2(1 + \frac{8}{3}\delta)]} \approx \sqrt{2}(1 + \frac{4}{3}\delta)$$

where the Nilsson deformation parameter  $\delta$  is used for description of oscillator frequencies. The  $O_2^+$  state with the energy  $\omega \approx 2\omega_0$  has not collective character. Remaining solutions characterise the position of corresponding branches of giant quadrupole resonance (GQR) in deformed nuclei. In the limit of zero deformation the solution  $\omega = \sqrt{2}\omega_0$  agrees very well with the experimental data on isoscalar GQR [6]. It must be noted that since this model used in this chapter is very simple the low-lying collective excitations of nuclei ( $\beta$  and  $\gamma$ -bands) are described quite well

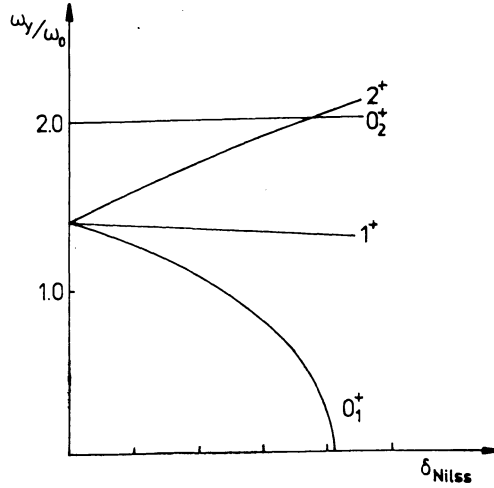


Fig. 2. Dependence of energies of giant quadrupole resonance components on deformation parameter  $\delta_{\text{Nilss}}$  in the nonrotating case ( $\Omega = 0$ ).

The dependence of energies of GQR states on deformation parameter in the nonrotating case ( $\Omega = 0$ ) is shown in fig. 2. One can see that the excitation energy of phonon state  $O_1^+$  monotonously decreases with increasing  $\delta$  and acquires zero values at  $\delta = 1/4(\sqrt{7} - 1) = 0.411$ . Further we restrict ourselves to investigation of model

characteristics in the region of  $\delta$  and  $\Omega$  where the phonon energies  $\hbar\omega$  are nonzero in the framework of RPA.

As was mentioned above in the region of rotational frequencies  $\Omega \cong \Omega_{cr}^{(1)}$  angular momentum is aligned along the symmetry axis and the projection of angular momentum onto this axis is a good quantum number. Further this projection will be assigned by symbol  $\tau$ . In this case secular equation for phonon energies can be also divided into three independent equations – two of them determine the excitation of positive signature with  $\tau = 0, \pm 2$  and the third one characterises the excitation of negative signature with  $\tau = \pm 1$ . We solved these equations with assumption of dependence of model strength constant  $g = 18\kappa C/m^2\omega_0^4$  on rotational frequency  $\Omega$ . This dependence was determined by requirement of exclusion of nonspherical spurious modes from solutions of motion equations. These spurious modes appear in the solutions of motion equation as a result of violation of rotational invariance of Hamiltonian by deformed average field (see [4, 5]). This requirement of exclusion has the following form

$$(19) \quad g = v_+ v_- .$$

Relation (19) together with the condition of selfconsistency (see [3]) determines wholly the function  $g(\Omega)$ . It must be noted that there are also alternative approaches for analysis of collective excitations in fast rotating nuclei (see e.g. [8] in which the strength constant are not dependent on rotational frequency).

If the quadrupole operator matrix elements are written in spherical coordinate system oriented with respect to symmetry axis the equations (15) for the states with  $\tau = 0$  can be expressed as

$$(20) \quad \frac{2}{3} (v_y - \lambda)^2 \left\{ \frac{2}{v_x(4v_x - v)} + \frac{1}{(v_y - \lambda)(4v_y - \lambda)} \right\} = 1$$

where  $g = 18\kappa C/m^2\omega_0^4$  and  $\lambda = \Omega^2/\omega_0^2$ . The constants  $C$  are given by condition of nuclear volume conservation

$$(21) \quad \langle x^2 \rangle \langle y^2 \rangle \langle z^2 \rangle = \frac{C^2}{m^3 \omega_x^2 \omega_y^2 \omega_z^2} .$$

The equation (20) has two solutions which are determined by

$$(22) \quad \begin{aligned} v &= a \pm \sqrt{a^2 - b} \\ a &= 2(v_x + v_y - g/3v_x - \sqrt{g/6}) \\ b &= 4(4v_x v_y - 4g v_y/3v_x - 2\sqrt{(g) v_x/3}) . \end{aligned}$$

Similarly one can obtain the equation

$$(23) \quad v^2 + 6\sqrt{(\lambda) v} + 10\lambda - 2v = 0$$



for the case of  $\tau = \pm 2$ . This equation has also two solutions

$$(24) \quad v_{1,2} = \pm 3\sqrt{\lambda} + \sqrt{(2\nu - \lambda)}.$$

Eventually the following equation holds for the negative signature ( $\tau = \pm 1$ ) states

$$(25) \quad z^3 - z \left[ 2 \left( 1 + \frac{\sqrt{\lambda}}{6} \right) + \frac{2\sqrt{\lambda} \left( 1 + \frac{2}{3}\sqrt{\lambda} \right)}{1 + \sqrt{\lambda}} \right] + \frac{2\sqrt{\lambda} \left( 1 + \frac{2}{3}\sqrt{\lambda} \right)}{1 + \sqrt{\lambda}} = 0$$

where  $z = \sqrt{\nu} + \sqrt{\lambda}$ . Since the analytical form of solution of this equation is not so clear we present here the approximate form obtained by expansion into the power series in  $\Omega$

$$(26) \quad \omega^{\tau=\pm 1} \approx \sqrt{2} \omega_0 + \frac{7}{6\sqrt{2}} \Omega \pm \frac{3}{2} \Omega$$

$$(27) \quad \omega_{prec}^{\tau=\pm 1} \approx \frac{3}{2} \frac{\Omega^2}{\omega} \left( 1 - \frac{8}{9} \frac{\Omega}{\omega_0} \right).$$

For comparison we give also and analogous expansions for positive signature solutions (22) and (24)

$$(28) \quad \omega^{\tau=0} \approx \begin{cases} 2\omega_0 \\ \sqrt{2} \omega_0 + \frac{5\sqrt{2}}{6} \Omega \end{cases}$$

$$\omega^{\tau=\pm 2} \approx \sqrt{2} \omega_0 - \frac{\Omega}{3\sqrt{2}} \pm 3\Omega.$$

The expressions (26)–(28) characterise the splitting of different branches of isoscalar GQR in rotating nucleus and (27) determines the frequency of low-energy precessional mode. Adiabatic estimate of frequency of precessional vibrations is (see [6])

$$(28') \quad \omega_{prec}^{adiab} = \Omega [(\Phi_x - \Phi_y)(\Phi_x - \Phi_z)/\Phi_y\Phi_z]^{1/2}$$

where  $\Phi_i$  are the rigid body values of moment of inertia with respect to corresponding axes. In the case of axial symmetric rotating nuclei this expression can be written as follows

$$(29) \quad \omega_{prec}^{adiab} = \Omega \frac{\nu_x - \nu_y + \lambda}{\nu_x + \nu_y + \lambda} \approx \frac{\Omega^2}{2\omega_0} \left( 1 - \frac{5}{6} \frac{\Omega}{\omega_0} + \dots \right).$$

This result differs substantially from our expression (27). For axial symmetric case  $\omega_{prec}^{\tau=\pm 1}/\omega_{prec}^{adiab} \approx 3$  for small values of rotational frequencies and this ratio decreases into about 2 in the region of higher rotational frequencies. It reaches the value near 2 also for nonaxial case.

### 2.2.2. Transition probabilities

As it was given in [1] the presence of signature of states determines the selection rules of states in transitions. According to these rules the states with positive signature have the even value of quantum number of angular momentum  $I$  and negative signature states correspond to odd values of  $I$ . The general expression for reduced transition probabilities is given in paper [1] (see rel. (74). For  $I \gg 1$  and for transitions from one-phonon states into the states in yrast line the rel. (74) in [1] can be rewritten as

$$(30) \quad \langle \alpha, \sigma, I \pm \tau | \hat{\mathcal{M}}(E\lambda) | yrI \rangle \approx \sqrt{(2I)} \langle \sigma, \alpha | \hat{\mathcal{M}}'(\lambda, m = \tau) | yrast \rangle .$$

Here  $\hat{\mathcal{M}}'(\lambda, m_x = \tau)$  is the component of intrinsic multipole moment with the projection  $\tau$  onto the rotational axis  $x$ . In the framework of RPA the intrinsic matrix element of the operator  $\hat{\mathcal{M}}$  is understood to have the following form

$$(31) \quad \langle \sigma, \alpha | \hat{\mathcal{M}}' | yrast \rangle = \langle \Omega | [O_{\alpha\sigma}, \hat{\mathcal{M}}] | \Omega \rangle = [O_{\alpha\sigma}, \hat{\mathcal{M}}]_{RPA}$$

where  $O_{\alpha\sigma}$  is the annihilation operator of phonon which is connected with the generalised coordinates  $\hat{X}_\alpha(o)$  and linear momenta  $\hat{\mathcal{P}}_\alpha(o)$  by (see rel. (30) in [1])\*

$$(31') \quad O_{\alpha\sigma}^+ = \frac{1}{\sqrt{2}} (\hat{X}_\alpha(\sigma) - i \hat{\mathcal{P}}_\alpha(\sigma)) .$$

The simplicity of spectrum in our simple model gives possibility to obtain almost total information on transitional probabilities from the analysis of sum rules for corresponding transitions. The example of such sum rule is represented by following relations

$$(32) \quad \sum_\alpha \omega_\alpha |\langle \alpha | \hat{Q}_{xx} | yr \rangle|^2 = \frac{2}{3} q^2 \left\{ 1 + \frac{1}{2} \frac{\langle yr | \hat{Q}_{xx} | yr \rangle}{\langle yr | \sum_{v=1}^A r_v^2 | yr \rangle} \right\}$$

$$\sum_\alpha \omega_\alpha |\langle \alpha | \hat{Q}_{xy} | yr \rangle|^2 = \frac{1}{2} q^2 \left\{ 1 - \frac{1}{2} \frac{\langle yr | \hat{Q}_{zz} | yr \rangle}{\langle yr | \sum_{v=1}^A r_v^2 | yr \rangle} \right\}$$

where  $q^2$  is given by

$$q^2 = \frac{6\hbar^2}{\sqrt{2} m\omega_0} \langle yr | \sum_{v=1}^A r_v^2 | yr \rangle$$

and  $\omega_\alpha$  is excitation energy in RPA expressed in the unit of  $\sqrt{2} \omega_0$ . The similar expression can be obtained from (32) by change of indices  $x, y$  and  $z$ .

\*) Since we are interested in phonons with  $\omega_\alpha \neq 0$  the energetical factors  $\sqrt{\omega_\alpha}$  and  $1/\sqrt{\omega_\alpha}$  in (30) of paper [1] is involved in definition of  $X_\alpha$  and  $\mathcal{P}_\alpha$ .

In the value of  $\omega_0 = 41A^{-1/3}$ ,  $\langle yr | \sum_{\nu} r_{\nu}^2 | yr \rangle = \frac{3}{5} 1.44A^{5/3} 10^{-26} \text{ cm}^2$  we have  $q^2 = 12.3A^{2/3} q_{weis}$  where  $q_{weis}$  is single-particle unit of quadrupole transition reduced probability.

The expressions for sum which obtain higher powers of  $\omega_{\alpha}$  are very complicated. We restrict ourselves into the analysis of (32) and also of sum involving the third order powers in  $\omega_{\alpha}$  which are presented below

$$(33a) \quad \sum_{\alpha} \omega_{\alpha}^3 |\langle \alpha | \hat{Q}_{xx} | yr \rangle|^2 = \frac{2\hbar^2}{m} \left\{ \langle yr | \sum_{\nu} (r_{\nu}^2 + 3x_{\nu}^2) | yr \rangle + \right. \\ \left. + \frac{1}{m^2 \omega_0^2} \langle yr | \sum_{\nu} (p_{\nu}^2 + 3(p_{\nu x})^2) | yr \rangle - \frac{2\kappa}{m\omega_0^2} [\langle yr | \sum_{\nu} (r_{\nu}^2 + 3x_{\nu}^2) | yr \rangle^2 + \right. \\ \left. + \langle yr | \sum_{\nu} (2r_{\nu}^2 - 3z_{\nu}^2) | yr \rangle^2 + \langle yr | \sum_{\nu} (2r_{\nu}^2 - 3y_{\nu}^2) | yr \rangle^2] \right\}$$

$$(33b) \quad \sum_{\alpha} \omega_{\alpha}^3 |\langle \alpha | \hat{Q}_{xy} | yr \rangle|^2 = \frac{9}{2} \frac{\hbar^2}{m} \left\{ \langle yr | \sum_{\nu} (x_{\nu}^2 + y_{\nu}^2) | yr \rangle + \right. \\ \left. + \frac{1}{m^2 \omega_0^2} [\langle yr | \sum_{\nu} ((p_{\nu x})^2 + (p_{\nu y})^2) | yr \rangle - 9\kappa m \langle yr | \sum_{\nu} (x_{\nu}^2 + y_{\nu}^2) | yr \rangle] \right\}.$$

In this case of  $\Omega = 0$  and  $\Omega \geq \Omega_{cr}^{(1)}$  when the shape of average nuclear field is axial symmetric the number of terms in sums (32), (33) is so small that the expressions above make possible to determine the most of matrix elements up to the phase factor.

According to (32), (33) calculated values of  $|\langle \alpha | Q_{2m} | \Omega = 0 \rangle|^2$  in nonrotating case  $\Omega = 0$  are presented in fig. 3 in dependence on deformation parameter  $\delta$ . The state  $O_2^+$  has noncollective character in all values of  $\delta$ . Matrix element  $|\langle O_1^+ | \hat{Q}_{20} | 0 \rangle|^2$  increases and energy  $\omega_{O_1^+}$  decreases with increasing deformation parameter  $\delta$  (see also fig. 2) so the partial sum of transition strength  $\sum_{\alpha} \omega_{\alpha} |\langle \alpha | \hat{Q}_{20} | 0 \rangle|^2$  doesn't change more than 40% in all interval of  $\delta$  where the solutions of  $G\hat{Q}R$  for  $O^+$  states exist.

In high rotational velocities  $\Omega \geq \Omega_{cr}^{(1)}$  the quadrats of matrix elements can be written in the following form

$$(34) \quad |\langle \tau, i | \hat{Q}_{\alpha\tau} | yr \rangle|^2 = \delta_{\tau\tau'} X_{\tau i}$$

where the additional index of state  $i$  runs over the two values ( $i = 1, 2$ ) in the case of  $\tau = 0, +1$  and is absent in  $\tau = \pm 2, -1$ . The values of  $X_{\tau i}$  can be obtained from (32), (33) using the formulae for average values given in [3]. As a result we obtain the following relations

$$(35) \quad X_{01}\varepsilon_1 + X_{02}\varepsilon_2 = q^2 A, \quad X_{01}\varepsilon_1^3 + X_{02}\varepsilon_2^3 = q^2 B \quad \text{for } \tau = 0$$

where  $i = 1$  corresponds to lower state and  $i = 2$  to upper one. Symbols  $\varepsilon_i$  ( $i = 1, 2$ ) stand for the energies of the states with  $\tau = 0$ .

$$(36) \quad A = \frac{2\sqrt{g} + v_x}{2v_x + \sqrt{g}}$$

$$B = \frac{\sqrt{g} v_x}{(2v_x + \sqrt{g})} \left\{ \frac{1}{v_x \sqrt{g}} (2\sqrt{g} + v_x) + \frac{1}{\sqrt{g}} (2\sqrt{g} + v) - \frac{1}{3} \left[ \frac{2\sqrt{g} + v_x}{v_x} \right]^2 \right\}$$

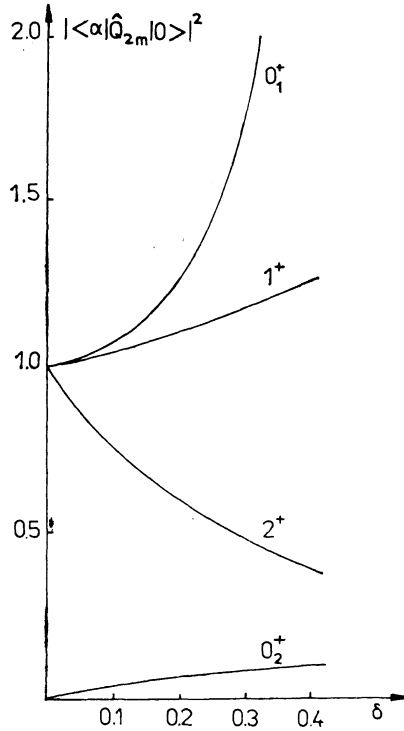


Fig. 3. Square values  $|\langle \alpha | \hat{Q}_{2m} | 0 \rangle|^2$  in dependence on deformation parameter  $\delta$  in the case of  $\Omega = 0$ .

The relations of sum rule can be written only for the operators proportional to Hermitian ones. Such operators are  $\hat{Q}_{2\tau} \pm \hat{Q}_{2-\tau}$  ( $\tau = 1, 2$ ). Choice of sign in this combination is arbitrary because the quadrats of matrix elements for both cases coincides. Defining the variables  $X_{\tau=2, i=1,2}$  as follows

$$(37) \quad X_{\tau=2, i=1,2} = \frac{1}{2} |\langle \tau = \pm 2 | \hat{Q}_{2\pm 2} | yr \rangle|^2$$

we obtain for corresponding quantities  $A$  and  $B$  the following expressions

$$(38) \quad A_{\tau=2} = \frac{3v_x}{2v_x + \sqrt{g}} \quad B_{\tau=2} = 3 \frac{(1 + \lambda) v_x}{2v_x + \sqrt{g}}$$

The estimate for the case  $\tau = +1$  can be also obtained from (32) and (33) neglecting the contribution of precessional mode. Eventually for  $\tau = +1$  we have

$$X_{\tau=1, i=1,2} = \frac{1}{2} |\langle \tau = \pm 1 | \hat{Q}_{2\pm 1} | yr \rangle|^2$$

$$(39) \quad A_{\tau=1} = \frac{3}{2} \frac{v_x + \sqrt{g}}{2v_x + \sqrt{g}}$$

$$B_{\tau=1} = \frac{3}{2} \left\{ 1 + \frac{v}{\sqrt{g}} + \left( \frac{1}{v_x} + \frac{1}{\sqrt{g}} \right) - \frac{g}{2} \left( \frac{1}{v_x} + \frac{1}{\sqrt{g}} \right) \right\} / \left( \frac{1}{\sqrt{g}} + \frac{2}{v_x} \right).$$

Quadrats of matrix elements (34) of quadrupole operators for  $\tau = 0, \pm 1, \pm 2$  are shown in fig. 4 as a functions of rotational frequency. States  $|\tau = 0_2^+\rangle$  with energy  $\approx 2\omega_0$  have noncollective character in all values of  $\Omega$ . The remain quadrupole modes of GQR are collective and their contribution to the sum of the first order in  $\omega_\alpha$  is approximately constant for all  $\Omega \leq \Omega_{cr}^{(2)}$ .

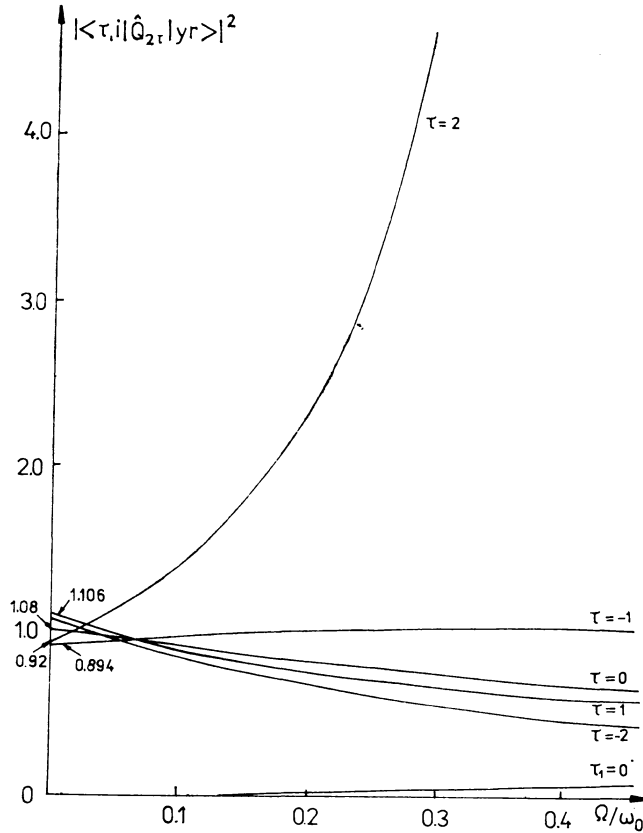


Fig. 4. Dependence of  $|\langle \tau, i | \hat{Q}_{2\tau} | yr \rangle|^2$  on rotational frequency  $\Omega$  for  $\tau = \pm 2, \pm 1, 0$ .

The general behaviour of reduced transition probabilities is in good agreement with the results of analysis of intrinsic matrix elements based on sum rules. Soft component of GQR ( $\tau = 2$ ) keeps its collective character in whole interval of  $\Omega$  ( $\Omega < \Omega_{cr}^{(2)}$ ). In values of  $\Omega \geq \Omega_{cr}^{(1)}$  this component has the sharp value of projection of angular momentum onto symmetry axis and the transitions connected with decreasing of phonon energy cause the decreasing of angular momentum by two Planck units.

Quite intensive transition probabilities occur between the yrast states and the states of precessional character. Calculations show that the dependence of such transition on angular momentum obtained in the framework of RPA has the different behaviour in comparison with the results of rigid rotor model. Some agreement of RPA results with the phenomenological rigid rotor model is observed for  $\Omega \geq 0.2\omega_0$ .

### 2.3. Isovector dipole resonance

As an example of negative parity residual interactions the isovector dipole forces are investigated in this part of paper (see also [9]). In this case  $H_{res}^{(-)}$  has the following form

$$(40) \quad H_{res}^{(-)} = \eta \sum_{i=x,y,z} \frac{m\omega_i^2}{2A} \left( \sum_{\nu=1}^A \tau_3(\nu) \hat{X}_i(\nu) \right)^2$$

where  $\tau_3(\nu)$  is the third component of isospin Pauli matrix  $\tau_3 = \begin{pmatrix} 1 & 0 \\ 0 & -1 \end{pmatrix}$  and  $\eta$  is the strength parameter characterising the isovector contribution of neutron and proton average field

$$(41) \quad V_n^p(\nu) = \frac{m}{2} \left( 1 \mp \eta \frac{N-Z}{A} \right) \sum_{i=x,y,z} \omega_i^2 x_i(\nu)^2.$$

The parametrization of dipole interaction (40) corresponds to the receipt of construction of effective residual forces restoring translation invariance of model Hamiltonian (see [1] and [10]). The concrete value of parameter  $\eta$  is usually determined from experimental data on position of giant dipole resonance (GDR) and reaches  $\eta \approx 3$  for oscillator potential.

The symmetry of average nuclear field with respect to  $R_x(\pi)$  transformation makes possible to divide  $H_{res}^{(-)}$  into two parts (see (11))

$$(42) \quad \begin{aligned} H_{(-)}^{(+)} &= \eta \frac{m\omega_x^2}{2A} \left( \sum_{\nu=1}^A \tau_3(\nu) \hat{X}(\nu) \right)^2 \\ H_{(-)}^{(-)} &= \eta \sum_{i=y,z} \frac{m\omega_i^2}{2A} \left( \sum_{\nu=1}^A \tau_3(\nu) \hat{X}_i(\nu) \right)^2. \end{aligned}$$

The solution of RPA equations of motion (40) can be found in analogous way as for quadrupole excitation using the scheme described in [1]. However sufficiently simple form of dipole interactions (42) enable to apply the simple alternative method. In this dipole case the RPA equations can be rewritten in the following form (we are interested only in nonspurious solutions)

$$(43) \quad [H_{s.p.} + H_{res}^(-), \mathcal{D}_\lambda^+] = \tilde{\omega}_\lambda \mathcal{D}_\lambda^+$$

where the dipole phonon creation operator  $\mathcal{D}_\lambda^+$  has the following structure

$$(44) \quad \mathcal{D}_\lambda^+ = \frac{1}{\sqrt{A}} \sum_{\nu=1}^4 \tau_3(\nu) a_\lambda^+(\nu).$$

Here  $a_\lambda(\lambda = +, -, x)$  are the operators of creation of oscillator quanta (see (5)). Substituting (44) into (41) we obtain for the spectrum of GDR frequencies

$$(45) \quad \begin{aligned} \tilde{\omega}_x &= \sqrt{(1 + \eta) \omega_x} \\ \tilde{\omega}_\pm^2 &= (1 + \eta) \frac{\omega_y^2 + \omega_z^2}{2} + \Omega^2 \pm \sqrt{[(1 + \eta)^2 (\omega_y^2 - \omega_z^2)^2 + 8\Omega^2 (1 + \eta) (\omega_y^2 + \omega_z^2)]}. \end{aligned}$$

The probabilities of electromagnetic transitions deexcitating the states of GDR with quantum numbers  $(\lambda, I)$  into the yrast line states are determined by following relation

$$(46) \quad |\tilde{X}_\lambda^\mu|^2 = |\langle yr | \mathcal{M}(E1, -\mu) \mathcal{D}_\lambda^+ | yr \rangle|^2 = |[\mathcal{M}(E1, -\mu), \mathcal{D}_\lambda^+]_{RPA}^2|$$

where

$$(47) \quad \mathcal{M}(E1, \mu) = \begin{cases} \sum_{\nu=1}^4 \tau_3(\nu) X(\nu) & \text{for } \mu = 0 \\ \mp \frac{1}{\sqrt{2}} \sum_{\nu=1}^4 \tau_3(\nu) (y(\nu) \pm i z(\nu))^2 & \text{for } \mu = \pm 1 \end{cases}$$

are the spherical components of dipole nucleus moment operator in the coordinate system where the quantum axis coincides with rotational axis. Using the results of paper [3] for the coefficients of transformation (6), it is possible to write the explicite expressions for transition amplitudes  $|\tilde{X}_\lambda^\mu|^2$

$$(48) \quad |\tilde{X}_\lambda^0|^2 = (2m\omega_x \sqrt{(1 + \eta)})^{-1} \text{ for } \lambda = x$$

$$(49) \quad \begin{aligned} |\tilde{X}_\lambda^{\pm 1}|^2 &= |Y_\pm \pm i Z_\lambda|^2 = \lambda \frac{\omega_\lambda^2 - \omega_z^2 + \Omega^2 / (1 + \eta)}{2m\omega_\lambda \sqrt{(1 + \eta) (\omega_\lambda^2 - \omega_z^2)}} \times \\ &\times \left\{ 1 \pm \frac{2\omega_x \Omega / \sqrt{(1 + \eta)}}{\omega_\lambda^2 - \omega_z^2 + \Omega^2 / (1 + \eta)} \right\} \text{ for } \lambda = \pm. \end{aligned}$$

Similarly as in the case of quadrupole excitations if the rotation is not present ( $\Omega = 0$ ) the dipole states can be classified by quantum number  $K^\pi$ . For longitudinal  $K^\pi = 0^-$  and transversal  $K^\pi = 1^-$  modes of dipole vibrations in this case we have

$$(50) \quad \begin{aligned} \tilde{\omega}(0^-) &= \sqrt{(1 + \eta)} \omega_z = \sqrt{(1 + \eta)} \omega_0 (1 - \frac{4}{3}\delta)^{1/2} \\ \tilde{\omega}(1^-) &= \sqrt{(1 + \eta)} \omega_\perp = \sqrt{(1 + \eta)} \omega_0 (1 + \frac{2}{3}\delta)^{1/2} \end{aligned}$$

Quadrants of intrinsic matrix elements of dipole moment operator for  $\Omega = 0$  determine the reduced dipole transition probability with corresponding final state  $K^\pi$ , so

$$(51) \quad B(E 1, 0^+ \rightarrow K^\pi) = \frac{q_1}{2m \tilde{\omega}(K^\pi)} \frac{1}{1 + \delta_{K0}}$$

where  $q_1 = 3A(e\hbar^2)/16\pi$ .

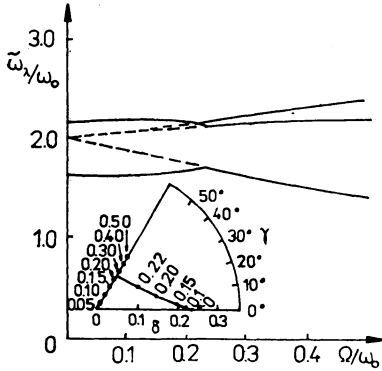


Fig. 5.

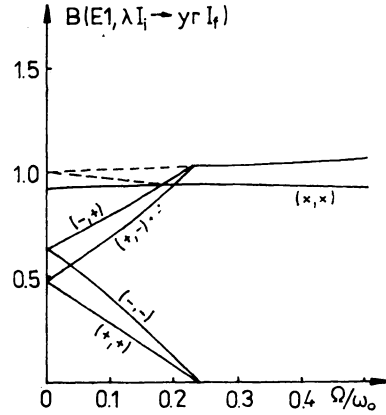


Fig. 6.

*Fig. 5.* Dependence of GDR component energy on rotational frequency  $\Omega$ . The figure includes also the diagram of deformation parameters  $\delta, \gamma$  as a function of  $\Omega$ . Dashed lines correspond to nucleus with spherical shape for  $\Omega = 0$  while the solid lines are connected with deformed nuclei for  $\Omega = 0$  ( $\delta = 0.25$  for  $\Omega = 0$ ) (see [9]).

*Fig. 6.* Dependence of reduced probabilities  $B(E 1, \lambda I_i \rightarrow \gamma I_f)$  for transitions of GDR into the yrast line states for different values  $\mu = I_i - I_f$ . The reduced probabilities are given in units  $q_1$ . The first symbol in brackets characterises the type of GDR state ( $\lambda = x, +, -$ ) and the second one corresponds to  $\mu = 0$  for  $\lambda = x$  and  $\mu = +1$  for  $\lambda = \pm$ .

Estimates of GDR splitting obtained above are in good agreement with experimental data on photoabsorption cross section [1]. In  $\Omega \neq 0$  case the additional splitting of frequencies of transverse dipole vibrations and a shift of longitudinal vibrations appear. Corresponding excitations are then classified by means of signature quantum number. In this simple model when the rotating nucleus obtains the axial symmetric oblate shape and rotational axis coincides with the symmetry axis



the additional splitting of negative signature dipole state occurs. This negative signature splitting can be characterised by additional quantum numbers  $\lambda = +1$  which correspond to the projection of phonon angular momentum  $\mu = \pm 1$  onto rotational axis.

The dependence of GDR energies on rotational frequency is shown in fig. 5. The figure includes also the diagram of deformation parameters  $\delta$ ,  $\gamma$  as a function  $\Omega$ . The dependence of reduced transition probabilities on  $\Omega$  is given in fig. 6. Selection rule with respect to signature

$$(52) \quad (-1)^I \sigma = 1$$

do not allow the dipole transition  $\lambda = x \rightarrow yr$  with the angular momentum change. In such a way the value of partial sum

$$(53) \quad \sum_{\lambda} \tilde{\omega}_{\lambda} |\langle yr | \hat{\mathcal{M}}(E 1, \mu = 0) | \lambda \rangle|^2 = \tilde{\omega}_{\lambda} |[\hat{\mathcal{M}}(E 1, 0), \mathcal{D}_{\lambda}]_{RPA}|^2 = \frac{q_1}{2m}$$

entirely determines the integral character of transitions without spin change. In rotation round the symmetry axis only the transitions ( $\lambda = \pm, I \pm 1 \rightarrow yr, I$ ) are possible. The reduced transition probability of such transitions are the same in all spins (see fig. 6) (if the occupation of states  $\lambda = \pm$  are equal). In the case of collective rotation the both type of dipole transitions ( $\lambda = \pm, I \rightarrow yr, I \pm 1$ ) and the behaviour of reduced probability of such transitions are shown in fig. 6 by solid lines. The sum rule with energy in the first order for these transitions is given by two components sum of which is practically the same as in the case (53) without spin change.

The model discussed in this chapter enables to investigate the properties of GDR and GQR in the process of nuclear rotation. In the framework of this model it is possible to describe the position and dependence of components of GDR and GQR on quadrupole deformation in nonrotating case. As was mentioned in [2] the Hamiltonian (4) also qualitatively reflects such important characteristics as the dependence of inertia moment on distribution of nuclear matter and appearance of nonaxiality in consequence of rotation. It must be noted that the changes of energies of different components of GDR is not so expressive as for GQR.

### 3. Application of cranking + RPA model for description of collective states of rotating nuclei

#### 3.1. Low lying states of $^{158}\text{Dy}$ and $^{168}\text{Er}$

In description of low-lying states we start with the Hamiltonian given in [1] in rel. (5)

$$(54) \quad H' = \sum_k e_k c_k^{\dagger} c_k - \frac{1}{4} \sum_{\tau} G_{\tau} P_{\tau}^{\dagger} P_{\tau} - \frac{1}{2} \sum_{\lambda=1,2,3\dots} \sum_{\mu=-\lambda}^{\lambda} \kappa_{\lambda} \hat{Q}_{\lambda\mu}^{\dagger} Q_{\lambda\mu}$$

where all symbols are described in [1]. We restrict ourselves by residual interaction with multipolarities  $\lambda = 1, 2, 3$ . Besides that the conditions of transition invariance gives the additional dipole-octupole interaction. It is well known fact (see e.g. [11]) that it is sufficient to take into account only isoscalar part of residual quadrupole-quadrupole and octupole-octupole interaction for description of low-lying quadrupole and octupole states. The important role in studying of  $E 1$ , transitions between low-lying states is played by low-lying tiles of isovector GDR. Therefore the Hamiltonian has the following form

$$(55) \quad H' = \sum_k e_k c_k^+ c_k - \frac{1}{4} \sum_{\tau} G_{\tau} P_{\tau}^+ P_{\tau} - \frac{1}{2} \sum_{m=-2}^2 \kappa_{2m} \hat{Q}_{2m}^+ Q_{2m} - \frac{1}{2} \sum_{\tau=0,1} \sum_{m=-1}^1 \kappa_{1m}^{[\tau]} Q_{1m}^{[\tau]+} \hat{Q}_{1m}^{[\tau]} \\ - \frac{1}{2} \sum_{m=-3}^3 \kappa_{3m} \hat{Q}_{3m}^+ \hat{Q}_{3m} - \frac{1}{2} \sum_{\tau=0,1} \sum_{m=-1}^1 \kappa_m^{[\tau]} [\hat{Q}_{1m}^{[\tau]+} \hat{Q}_{3m}^{[\tau]} + \hat{Q}_{3m}^{[\tau]+} \hat{Q}_{1m}^{[\tau]}]$$

where in opposite to (54) the dependence of strength constants  $\kappa_{\lambda\mu}$  and  $x_{\mu}$  on projection  $\mu$  is introduced ( $\kappa_{\lambda\mu} = \kappa_{\lambda-\mu}$ ,  $x_{\mu} = x_{-\mu}$ ). Here  $\kappa_{\lambda\mu}^{[0]}$  and  $\kappa_{\lambda\mu}^{[1]}$  are the isoscalar and isovector strength constants, respectively. In solving the RPA equations for Hamiltonian (55) we approximate the average field by axial symmetric deformed potential of Saxon-Woods form with parameters taken from refs. [12, 13]. The parameters of deformation were obtained by means of the method of Strutinsky [14]:  $\beta_2 = 0.265$ ,  $\beta_4 = 0.044$  for  $^{158}\text{Dy}$  and  $\beta_2 = 0.284$ ,  $\beta_4 = -0.001$  for  $^{168}\text{Er}$ . The deformed field violates the symmetry condition (4) and (5) in [1]. However the restoration of these symmetries according to receipt described in [1] leads to the complex dependence of the residual interaction on nucleon coordinates. Therefore fixing the residual interactions in the form of (55) only the strength constants  $\kappa_{\lambda\mu}$  and  $x_{\mu}$  can be determined from the requirement of validity of the symmetry conditions (4) in [1] in average.

The solving of RPA equation of motion was performed according to the method described in [1]. It is known (see e.g. [15]) that the method of Hartree-Fock Bogolubov without projection onto the particle number for cranking Hamiltonian in the region of rotational frequency doesn't give the good results when pairing vanishes. Since the pairing gap starts to decrease in spins  $I \sim 8\hbar$  for  $^{168}\text{Er}$  and  $I \sim 6\hbar$  for  $^{158}\text{Dy}$  the calculation of spectrum was performed up to spins  $I \leq 8\hbar$  and  $I \leq 6\hbar$  for these nuclei.

The dependence of spin  $I$  on rotational frequency in the states of yrast line is determined by the standart way the equations of Hartree-Fock-Bogolubov are solved in some increasing values of rotational frequency and simultaneously the expectation value  $\langle \Omega | I_x | \Omega \rangle$  is calculated. Using the cranking conditions  $\langle \Omega | I_x | \Omega \rangle = \sqrt{[I(I+1)]}$  the function  $I(\Omega)$  is obtained.

Solving Hartree-Fock-Bogolubov equations and taking into account the symmetries of single-particle operators involved in (55) (see appendix in [1]) the cranking Hamiltonian  $H'$  can be rewritten in the form (see (20) in [1]).

$$(56) \quad H' = \langle \Omega | H | \Omega \rangle + H_{(+)}^{(+)} + H_{(-)}^{(+)} + H_{(+)}^{(-)} + H_{(-)}^{(-)}$$

where

$$\begin{aligned} H_{(+)}^{(+)} &= \sum_{\mu} E_{\mu} b_{\mu}^{+} b_{\mu} - \frac{1}{2} \sum_{\tau} G_{\tau} \hat{P}_{\tau}^{(+)}(1) \hat{P}_{\tau}(1) - \frac{1}{2} \sum_{m=0}^2 \kappa_{2m} \hat{Q}_m^{(+)}(1) \hat{Q}_m^{(+)}(1) \quad (\mu = ik) \\ H_{(+)}^{(-)} &= \sum_{\nu} \frac{1}{2} E_{\nu} b_{\nu}^{+} b_{\nu} - \frac{1}{2} \sum_{m=1}^2 \kappa_{2m} \hat{Q}_m^{(-)}(1) \hat{Q}_m^{(-)}(1) \quad (\nu = ik \text{ and } i\bar{k}) \\ H_{(-)}^{(+)} &= \sum_{\mu} E_{\mu} b_{\mu}^{+} b_{\mu} - \frac{1}{2} (\kappa_{11}^{[01]} + \kappa_{11}^{[11]}) \wedge \mathcal{D}_1^{(+)}(1) \wedge \mathcal{D}_1^{(+)}(1) - \\ &- (\kappa_{11}^{[01]} - \kappa_{11}^{[11]}) \wedge \mathcal{D}_{1(neut)}^{(+)}(1) \wedge \mathcal{D}_{1(prot)}^{(+)}(1) - \frac{1}{2} \sum_{m=1}^3 \kappa_{3m} \hat{F}_m^{(+)}(1) \hat{F}_m^{(+)}(1) - \\ &- (\kappa_{11}^{[01]} + \kappa_{11}^{[11]}) \wedge \mathcal{D}_1^{(+)}(1) \wedge \mathcal{F}_1^{(+)} - \\ &- (\kappa_{11}^{(0)} - \kappa_{11}^{(1)}) \wedge \mathcal{D}_{1(neut)}^{(+)}(1) \hat{F}_{1(prot)}^{(+)}(1) + \wedge \mathcal{D}_{1(prot)}^{(+)}(1) \hat{F}_{1neut}^{(+)}] \\ H_{(-)}^{(-)} &= \frac{1}{2} \sum_{\nu} E_{\nu} b_{\nu}^{+} b_{\nu} - \frac{1}{2} \sum_{m=0,1} (\kappa_{1m}^{[01]} + \kappa_{1m}^{[11]}) \wedge \mathcal{D}_m^{(-)}(1) \wedge \mathcal{D}_m^{(-)}(1) - \\ &- \sum_{m=0,1} (\kappa_{1m}^{[01]} - \kappa_{1m}^{[11]}) \wedge \mathcal{D}_{m(neut)}^{(-)} \wedge \mathcal{D}_{m(prot)}^{(-)} - \\ &- \frac{1}{2} \sum_{m=0}^3 \kappa_{3m} \hat{F}_m^{(-)}(1) \hat{F}_m^{(-)}(1) - \sum_{m=0,1} (\kappa_{1m}^{[01]} + \kappa_{1m}^{[11]}) \wedge \mathcal{D}_m^{(-)}(1) \hat{F}_m^{(-)}(1) - \\ &- \sum_{m=0,1} (\kappa_{1m}^{[01]} - \kappa_{1m}^{[11]}) [\wedge \mathcal{D}_{m(neut)}^{(-)}(1) \hat{F}_{m(prot)}^{(-)}(1) + \wedge \mathcal{D}_{m(prot)}^{(-)}(1) \hat{F}_{m(neut)}^{(-)}(1)]. \end{aligned}$$

Here the indices  $m(neut)$  and  $m(prot)$  means the summation only over the neutron and proton two-quasiparticle states which contribute to linear boson part of given operator (see appendix of [1]). In all other cases the summation goes through the both proton and neutron components. The extraction of spurious modes and solving equation of motion for each of parts of Hamiltonian given above is performed in accordance with the method described in [1]. The dimensions of corresponding system of equations for Hamiltonian  $H_{(+)}^{(+)}$ ,  $H_{(+)}^{(-)}$ ,  $H_{(-)}^{(+)}$ ,  $H_{(-)}^{(-)}$  are 7, 2, 6, 10, respectively. Their explicit forms can be found in [16]. The existence of spurious mode  $\theta_x(1)$ ,  $I_x(1)$  (see [1]) among the solutions of RPA equations for Hamiltonian  $H_{(+)}^{(+)}$  allows to determine the inertia moment with respect to  $x$ -axis (see (32) and (65) in [1]). Since the corresponding expression is very complex we don't present it here (see [16]). The analogous expression can be obtained also for  $g_{N_x}$ . From requirement for the mode  $(X(1), P_x(1))$  to have the zero solution of RPA equation for Hamiltonian  $H_{(-)}^{(+)}$  we have obtained the expression for mass parameter  $g_{P_x}$  (see (34) in [1])

$$(58) \quad g_{P_x} = \frac{1}{M} = \frac{1}{2} \frac{S(0)_{F_2^{(+)}F_2^{(+)}} - 1/2\kappa_{32}}{[S_{F_2^{+}}(0)_{F_2^{+}} - 1/2\kappa_{33}] S_{P_x P_x}(0) - S_{F_2^{+}P_x}(0)}$$

where the quantity  $S_{AB}$  is given in (16) (see also definition (47) in [1]). From the symmetry of one-phonon wave function of Hamiltonian (57) it follows that the

even values of total angular momentum  $I$  correspond to solutions of RPA equation with Hamiltonians  $H_{(\pm)}^{(+)}$  while the odd values of  $I$  are connected with Hamiltonians  $H_{(\pm)}^{(-)}$ .

The experimental values of excitation energies (one-phonon rotational bands above yrast line) were compared with the values calculated according following formulae

$$(59) \quad E_{\lambda}(I) = E_{yr}(I_0) + \frac{\hbar^2}{2 \Phi_x(I_0)} [I(I+1) - I_0(I_0+1)] + \hbar \omega_{\lambda}(I_0)$$

where  $I = I_0$  for even values of spins and  $I = I_0 \pm 1$  for odd values of spins,  $\hbar \omega_{\lambda}(I_0)$  is the energy of one-phonon state  $O_{\lambda}^{+}(\pm)/\Omega_{I_0}$  and  $\Phi_x(I_0)$  is inertia moment. It must be noted that this expression is more precise for higher spins. In the low-spin region one has to correct the rel. (59) in the sense of comments given in [16].

The result of calculations depend obviously on strength constants. The values of strength constants were determined from following requirements

- i) the validity of translation and rotation invariance of total Hamiltonian which leads to the self-consistent conditions (41) in [1] (concrete form is given in [16]);
- ii) since the number of equations obtained from translation and rotation invariance of total Hamiltonian is less than the number of strength constants involved in Hamiltonian (57) some of the strength constants were determined from comparison of experimental and theoretical energies of some one-phonon states.

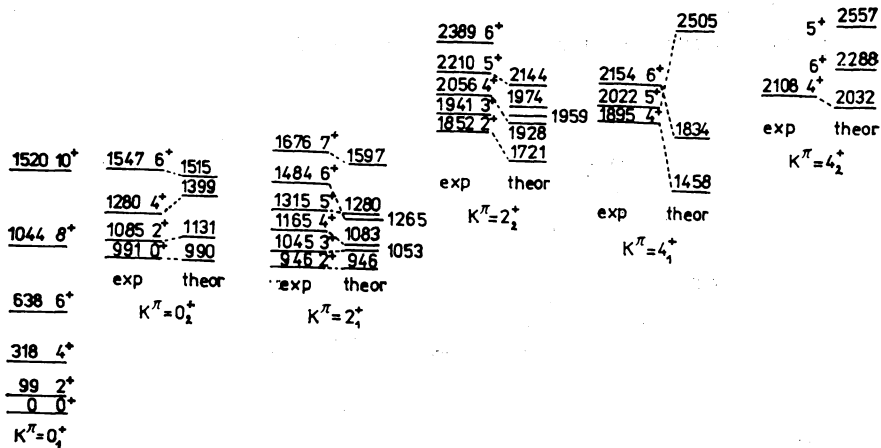


Fig. 7. Comparison of calculated experimental energies of positive parity low-lying states in  $^{158}\text{Dy}$ .

The more detailed informations about the strength constants are given in [16]. The comparison of theoretical and experimental spectrum is shown in figs. 7, 9 for  $^{158}\text{Dy}$  and figs. 8, 10 for  $^{168}\text{Er}$ . The theoretical values of  $B(E2)$  transitions in  $^{168}\text{Er}$  and  $^{158}\text{Dy}$  obtained from expressions (85)–(88) in [1] are compared with experimental ones in tables 1 and 2. The effective charges were taken in accordance

with [17]:  $e_{eff}^{\lambda=2} = 0.2$  for neutrons and  $e_{eff}^{\lambda=2} = 1.2$  for protons. The absolute values of  $B(E2)^{exp}$  were obtained from relative values  $B(E2)^{theor}$  by means of Alaga rules for intraband transitions supposing that intrinsic quadrupole moment  $Q_0$  for given rotational band is the same as the moment of ground state [18]. In cases when among  $E2$ -transitions from given state were no intraband transitions only relative values of  $B(E2)$  values were shown in tables 1 and 2. One can see that the better

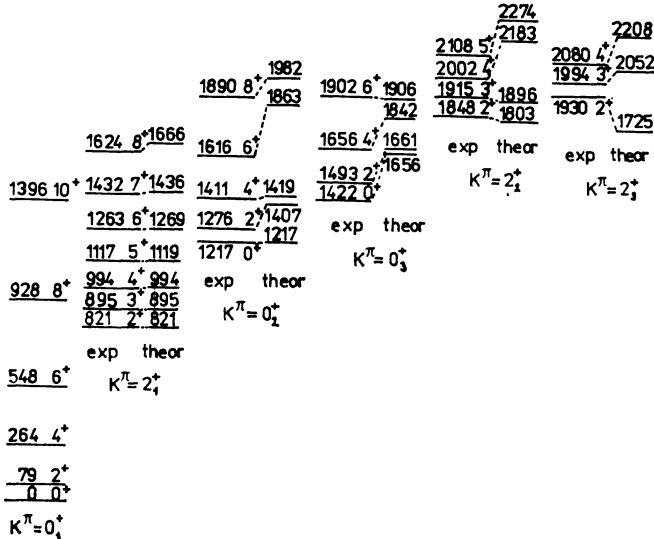


Fig. 8. Comparison of calculated and experimental energies of positive parity low-lying states in  $^{168}\text{Er}$ .

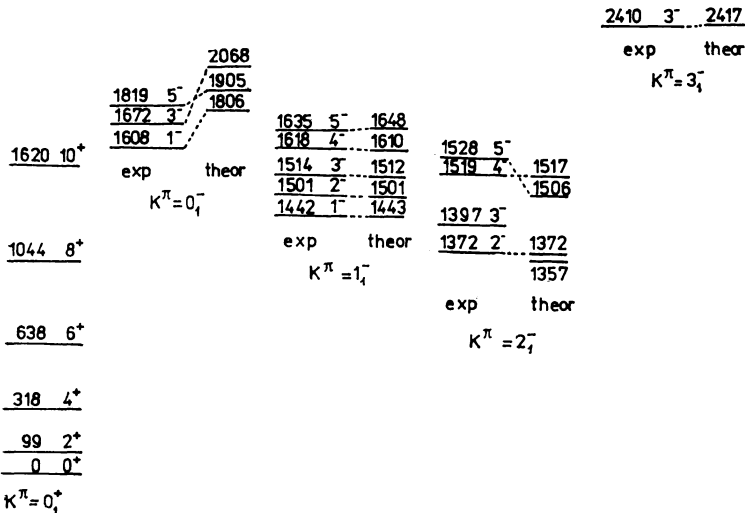


Fig. 9. Comparison of calculated and experimental energies of negative parity low-lying states in  $^{158}\text{Dy}$ .

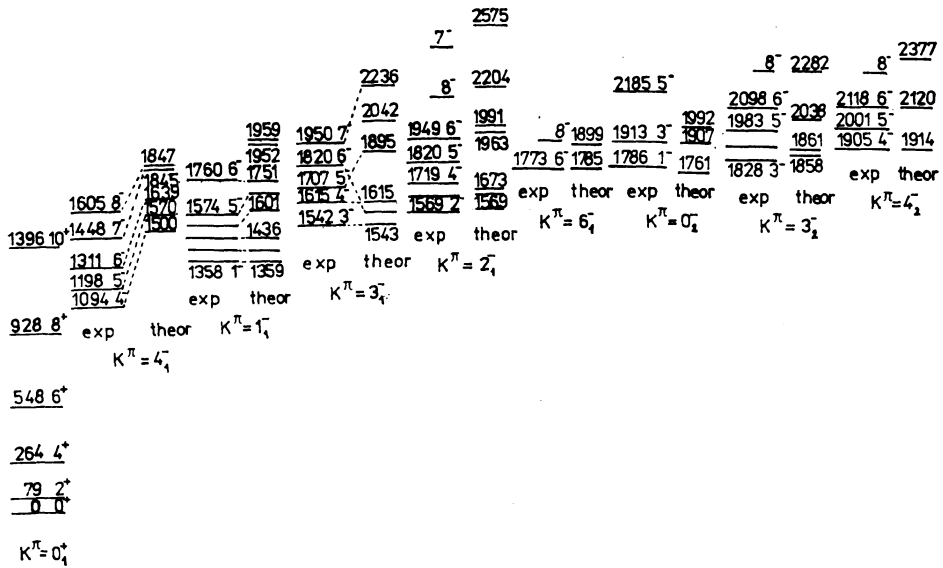


Fig. 10. Comparison of calculated and experimental energies of negative parity low-lying states in  $^{168}\text{Er}$ .

agreement with experimental  $B(E 2)$  values occurs in case of  $^{158}\text{Dy}$ . It is probably caused by quite big anharmonic effects in  $^{168}\text{Er}$  which is discussed e.g. in papers [18, 19]. However to take into account this anharmonicity it means to go beyond the RPA. It is interesting that used model reflected the fact of reduction of about two orders of  $B(E 2)$  values for transitions from  $\gamma$  – band into ground band for  $^{618}\text{Er}$  in comparison with  $^{158}\text{Dy}$ .

Table 1. Reduced transition probabilities  $B(E 2; I_i K_i \rightarrow I_f K_f)$  in  $^{168}\text{Er}$

1	2	3	4	5	6
$I_i K_i$	$I_f K_f$	$B(E 2)_{if}^{\text{exp}}$ $e^2 \cdot fm^4$	$B(E 2)_{if}^{\text{exp}}$ relat.	$B(E 2)_{if}^{\text{theor}}$ $e^2 \cdot fm^4$	$B(E 2)_{if}^{\text{theor}}$ relat.
1	2	3	4	5	6
$22_1^+$	$00_1^+$	259.2	54.1	163.8	34.3
	$20_1^+$	479.2	100,0	477,6	100,0
	$40_1^+$	32.6	6,8	166.7	34.9
$32_1^+$	$20_1^+$	533.5	100,0	113.0	100.0
	$40_1^+$	348.8	65.4	42.6	37.7

Table 1. (Continued)

42 <sub>1</sub> <sup>+</sup>	20 <sub>1</sub> <sup>+</sup>	108.4	1.6	117.3	1.5
	40 <sub>1</sub> <sup>+</sup>	551.4	8.1	427.4	5.6
	60 <sub>1</sub> <sup>+</sup>	75.9	1.1	140.4	1.8
	22 <sub>1</sub> <sup>+</sup>	6839.9	100.0	7633.9	100.0
52 <sub>1</sub> <sup>+</sup>	40 <sub>1</sub> <sup>+</sup>	315.9	2.9	405.1	3.3
	60 <sub>1</sub> <sup>+</sup>	394.3	3.6	232.6	1.9
	32 <sub>1</sub> <sup>+</sup>	10968.7	100.0	12241.8	100.0
62 <sub>1</sub> <sup>+</sup>	40 <sub>1</sub> <sup>+</sup>	59.9	0.4	52.5	0.35
	60 <sub>1</sub> <sup>+</sup>	515.9	3.8	76.8	0.5
	80 <sub>1</sub> <sup>+</sup>	183.7	1.4	43.7	0.29
	42 <sub>1</sub> <sup>+</sup>	13499.9	100.0	15071.7	100.0
72 <sub>1</sub> <sup>+</sup>	60 <sub>1</sub> <sup>+</sup>	184.6	1.2	1090.9	6.5
	80 <sub>1</sub> <sup>+</sup>	502.0	3.3	296.1	1.8
	52 <sub>1</sub> <sup>+</sup>	15152.9	100.0	16917.1	100.0
82 <sub>1</sub> <sup>+</sup>	60 <sub>1</sub> <sup>+</sup>	291.0	1.8	165.9	0.9
	80 <sub>1</sub> <sup>+</sup>	825.1	5.1	705.9	3.9
	62 <sub>1</sub> <sup>+</sup>	16295.0	100.0	18194.7	100.0
20 <sub>2</sub> <sup>+</sup>	00 <sub>1</sub> <sup>+</sup>	2.7	28.1	3.2	39.5
	20 <sub>1</sub> <sup>+</sup>	6.9	71.9	1.2	14.8
	40 <sub>1</sub> <sup>+</sup>	9.6	100.0	8.1	100.0
40 <sub>1</sub> <sup>+</sup>	20 <sub>1</sub> <sup>+</sup>	3.0	0.018	0.6	0.003
	40 <sub>1</sub> <sup>+</sup>	4.1	0.025	1.3	0.007
	60 <sub>1</sub> <sup>+</sup>	33.7	0.205	8.2	0.045
	20 <sub>1</sub> <sup>+</sup>	1615.7	100.0	1820.2	100.0
60 <sub>2</sub> <sup>+</sup>	40 <sub>1</sub> <sup>+</sup>	2.6	0.014	1.6	0.008
	60 <sub>1</sub> <sup>+</sup>	18.0	0.100	8.7	0.043
	80 <sub>1</sub> <sup>+</sup>	12.9	0.071	2.9	0.014
	40 <sub>1</sub> <sup>+</sup>	18080.2	100.0	2184.5	100.0
80 <sub>2</sub> <sup>+</sup>	60 <sub>1</sub> <sup>+</sup>	100.6	1.614	156.1	0.739
	80 <sub>1</sub> <sup>+</sup>	no exp. data	—	219.1	1.037
	60 <sub>1</sub> <sup>+</sup>	6234.6	100.0	21132.2	100.0

Table 2. Reduced transition probabilities  $B(E 2; I_i K_i \rightarrow I_f K_f)$  in  $^{158}\text{Dy}$

$I_i K_i$	$I_f K_f$	$B(E 2)_{if}^{\text{exp}}$ $e^2 \cdot \text{fm}^4$	$B(E 2)_{if}^{\text{exp}}$ relat.	$B(E 2)_{if}^{\text{theor}}$ $e^2 \cdot \text{fm}^4$	$B(E 2)_{if}^{\text{theor}}$ relat.
$22_1^+$	$00_1^+$	298.0	30.0	198.3	20.0
	$20_1^+$	983.1	100.0	945.3	100.0
	$40_1^+$	18.5	1.5	10.7	1.14
$32_1^+$	$20_1^+$	—	100.0	14.5	100.0
	$40_1^+$	—	70.3	8.7	60.4
$42_1^+$	$20_1^+$	—	12.0	80.1	9.12
	$40_1^+$	—	100.0	878.0	100.0
	$60_1^+$	—	13.6	69.6	7.93
$52_1^+$	$40_1^+$	304.0	3.3	482.4	4.4
	$60_1^+$	479.0	5.2	246.4	2.2
	$32_1^+$	9172.7	100.0	10993.2	100.0
$20_1^+$	$00_1^+$	106.0	17.3	94.2	8.91
	$20_1^+$	179.0	19.3	96.6	9.2
	$40_1^+$	611.8	100.0	1055.5	100.0
$40_1^+$	$20_1^+$	—	19.0	56.7	15.8
	$40_1^+$	—	16.8	73.4	17.3
	$60_1^+$	—	100.0	423.3	100.0
$32_1^+$	$20_1^+$	—	3.9	0.01	6.8
	$40_1^+$	—	100.0	0.16	100.0
$42_2^+$	$20_1^+$	—	24.6	3.26	24.9
	$40_1^+$	—	60.4	4.51	49.7
	$60_1^+$	—	100.0	9.08	100.0
$62_2^+$	$40_1^+$	—	80.4	0.18	77.2
	$60_1^+$	—	100.0	0.23	100.0
$44_1^+$	$20_1^+$	—	5.2	0.39	7.98
	$40_1^+$	—	100.0	4.88	100.0



Table 3. Ratio  $B(E 1, IK_v \rightarrow I + lgr)/B(E 1, IK_i \rightarrow I - lgr)$  in  $^{168}\text{Er}$

IK	Exp.	Theor. <sup>a)</sup>	Theor. <sup>b)</sup>
$10_2^-$	1.5295	0.0969	1.1879
$30_2^-$	1.2500	0.0360	0.3834
$11_1^-$	2.3793	20.0475	0.8970
$31_1^-$	0.9774	0.00014	2.9298
$51_1^-$	0.5691	0.1305	5.2117
$11_2^-$	0.1667	13.1670	—
$31_2^-$	0.2813	481.6754	—
$51_2^-$	0.9500	20.3880	—

<sup>a)</sup> Results of this paper.

<sup>b)</sup> Results of paper [20]

Table 4. Ratio  $B(E 1, IK_v \rightarrow I + lgr)/B(E 1, IK_i \rightarrow I - lgr)$  in  $^{158}\text{Dy}$

IK	Exp.	Theor. <sup>a)</sup>	Theor. <sup>b)</sup>
$10_2^-$	3.7850	27.8780	1.0445
$11_1^-$	0.8491	477.3660	1.0031
$31_1^-$	0.4167	4.2493	3.7429
$32_1^-$	0.3095	3.3890	1.9101
$33_1^-$	1.3763	0.5450	0.5147

<sup>a)</sup> Results of this paper.

<sup>b)</sup> Results of paper [20].

The comparison of theoretical and experimental ratios  $B(E 1, I_v \rightarrow I + 1\gamma) : B(E 1, I_v \rightarrow I - 1\gamma)$  is demonstrated in tables 3 and 4. These values are compared further with the results of paper [20] obtained from pure phenomenological model [21]. We used the following values of effective charges:  $e_{eff}^{\lambda=1} = -0.405$ ,  $e_{eff}^{\lambda=3} = 0.2$  for neutrons ( $^{168}\text{Er}$ ),  $e_{eff}^{f=1} = 0.595$ ,  $e_{eff}^{\lambda=3} = 1.2$  for protons ( $^{168}\text{Er}$ ),  $e_{eff}^{\lambda=1} = -0.418$ ,  $e_{eff}^{\lambda=3} = 0.2$  for neutrons ( $^{158}\text{Dy}$ ),  $e_{eff}^{\lambda=1} = 0.582$ ,  $e_{eff}^{\lambda=3} = 1.2$  for protons ( $^{158}\text{Dy}$ ). It can be seen from tables 3, 4 the agreement of  $E 1$ -transition probabilities is worse than for  $E 2$ -transitions. The  $E 1$ -transition probabilities are more sensitive to anharmonic effects which were not taken into account in RPA. We also neglected the errors caused by mixing of states with different signature in the low-spin region.

### 3.2. Alignment of octupole states in actinides

The properties of the low-lying octupole vibrational states in the actinide nuclei (see e.g. [22]) differ much from what could be expected from the adiabatically slow rotation. With increasing rotation, the vibrational angular momentum tends to align the direction of the rotational angular momentum, giving rise to distortion in the spectra of rotational states and to the new regularities in the transitions from the aligned states to the ground band states. These new features of the rotational band have been understood in the framework of a phenomenological model including the pure boson (octupole) operators coupled to a rotor by the Coriolis force [21, 23]. The conclusions of refs. [21, 23] were checked within the microscopic cranking + RPA model [24, 25]. In these papers the alignment of octupole phonons in the state of  $K^\pi = 0^-$  band in three nuclei  $^{230,232}\text{Th}$  and  $^{238}\text{U}$  was investigated. The alignment was studied also in ref. [26]. However, our Hamiltonian differs in parametrization from one considered in ref. [26].

The states of  $K^\pi = 0^-$  band are related to the states of negative signature. So our starting Hamiltonian was (see (20) in ref. [1])

$$H_{(-)}^{(-)} = \frac{1}{2} \sum_{ik} (E_{ik} b_{ik}^+ b_{ik} + E_{ik} b_{ik}^+ b_{ik}) - \frac{1}{2} \sum_{\tau\tau'} \kappa_{\tau\tau'} \sum_{m=0}^3 \hat{F}_m^{(-)}(\tau) \hat{F}_m^{(-)}(\tau')$$

where the notation is the same as in [1]. The separable octupole-octupole interaction contains both isoscalar and isovector component with the corresponding strength constants

$$(61) \quad \begin{aligned} 2\kappa_0 &= \kappa_{pp} + \kappa_{np} \quad (\kappa_{nn} = \kappa_{pp}) \\ 2\kappa_1 &= \kappa_{pp} - \kappa_{np} \end{aligned}$$

( $\tau = p$  (protons) or  $n$  (neutrons)).

Solving RPA equations of motion with Hamiltonian (60) for each value of rotational frequency  $\Omega_I$  corresponding to spin  $I$  in yrast line (using the receipt in [1]) we obtain the energy  $\hbar\omega_k$  and the structure of corresponding one-phonon state  $O_\alpha^+ |\Omega_I\rangle$ , that means the coefficients  $X_{ij}(X_{ij})$  and  $\mathcal{P}_{ij}(\mathcal{P}_{ij})$  of phonon creation operator

$$(62) \quad \begin{aligned} O_\alpha^+ &= \frac{1}{\sqrt{2}} (\hat{X}_\alpha - i \wedge \mathcal{P}_\alpha) = \frac{1}{\sqrt{2}} \sum_{ij} [(X + \mathcal{P}_{ij}^\tau) b_{ij}^+ + (X + \mathcal{P}_{ij}^\tau) b_{ij}^+ + \\ &+ (X - \mathcal{P}_{ij}^\tau) b_{ij} + (X - \mathcal{P}_{ij}^\tau) b_{ij}]. \end{aligned}$$

With these creation operators we can calculate aligned vibrational angular momentum  $i_\alpha(\Omega)$

$$(63) \quad i_\alpha(\Omega) = \langle \Omega_I | O_\alpha I_x O_\alpha^+ | \Omega_I \rangle - \langle \Omega_I | I_x | \Omega_I \rangle.$$

The phonon energies  $\omega_\alpha(I)$  and aligned vibrational momentum  $i_\alpha(\Omega)$  (63) should be compared with corresponding experimental values which can be extracted from experimental data according to the following receipt.

Let us define the energy of the state  $\alpha$  in the rotating frame

$$(64) \quad R_\alpha(\Omega) = E_\alpha(\Omega) - \Omega I_x^\alpha(\Omega)$$

where  $E_\alpha(\Omega)$  is the experimental energy of the excitation state  $\alpha$  for given rotational frequency  $\Omega$ ,  $I_x^\alpha(\Omega) = \langle \Omega_I | O_\alpha I_x O_\alpha^+ | \Omega_I \rangle$  is the angular momentum projection onto rotational axis (axis  $x$ ). The difference  $\omega_\alpha(\Omega) = R_\alpha(\Omega) - R_{yrast}(\Omega)$  is the experimental excitation energy of the state  $\alpha$  relative to the yrast line in the rotating frame, that means the quantity which should be compared with the phonon energy. With respect to (64) we have

$$(65) \quad \omega_\alpha(\Omega) = R_\alpha(\Omega) - R_{yrast} = E_\alpha(\Omega) - E_{yrast}(\Omega) - \Omega i_\alpha(\Omega).$$

In (65)  $i_\alpha(\Omega)$  is understood to be experimental value of aligned momentum.

The reduced probabilities of  $E 1$ -transitions from one-phonon octupole states  $\alpha$  to the states of yrast line can be calculated by means of the expressions (85)–(88) in [1]. From the point of view of comparison of experimental data on transition probabilities it is convenient to calculate the branching ratio

$$(66) \quad R_I = \frac{B(E 1, I_{OCT}^- \rightarrow (I-1)^+ yrast)}{B(E 1, I_{OCT}^- \rightarrow (I+1)^+ yrast)}$$

which is very sensitive to the structure of the wave function of the state. Substituting the expressions (85)–(88) from [1] into (66) we obtain

$$(67) \quad R_I = \frac{I}{I+1} \frac{|1 + Z \sqrt{[(I+1)/I]}|^2}{|1 - Z \sqrt{[I/(I+1)]}|^2}.$$

Here, the quantity

$$(68) \quad Z = \frac{\sum_{\tau\mu} e_\tau X_\mu^\tau \mathcal{W}_\mu^{(+)}(\tau)}{\sum_{\nu\mu} e_\nu P_\mu^\nu \mathcal{W}_\mu^{(-)}(\nu)}$$

is the microscopic image of the parameter introduced in ref. [27]. In (68)  $X_\mu^\tau = X_{ij}^\tau(X_{ij}^\tau)$ ,  $P_\mu^\nu = P_{ij}^\nu(P_{ij}^\nu)$ ,  $\mathcal{W}_\mu^{(\pm)}(\tau) = \mathcal{W}_{ij}^{(\pm)}(\tau)(\mathcal{W}_{ij}^{(\pm)}(\tau))$  and the operators  $\mathcal{W}_\mu^{(\pm)}$  are defined as follows

$$(69) \quad \begin{aligned} \hat{\mathcal{W}}^{(-)} &= \frac{1}{\sqrt{2}} (\hat{Q}_{11} - \hat{Q}_{1-1}) \\ \hat{\mathcal{W}}^{(+)} &= \frac{i}{\sqrt{2}} (\hat{Q}_{11} + \hat{Q}_{1-1}) \\ \hat{Q}_{1m}(\tau) &= \sum_{k=1}^{N_\tau} r_k Y_{1m}(\theta_k^\tau). \end{aligned}$$

Effective charges  $e_p = eN/A$  and  $e_n = -eZ/A$  have their standard dipole values.

In our calculations quasi-particle energies  $E_{ik} = E_i + E_k$  and corresponding two-quasi-particle boson operators  $b_{ik}$  (see (60)) were obtained by solving the Hartree-Fock-Bogolubov problem with the Nilsson Hamiltonian including the cranking term and the monopole pairing. We restrict ourselves into the spherical oscillator shells  $N = 4, 5, 6$  for protons and  $N = 5, 6, 7$  for neutrons. The parameters of deformation ( $\varepsilon_2, \varepsilon_4$ ), of the gap ( $\Delta$ ) and the chemical potential ( $\lambda$ ) are taken from refs. [28, 29] and kept constant. This approximation provides an excellent description of the properties of the yrast levels in the entire deformed actinide region [28–30].

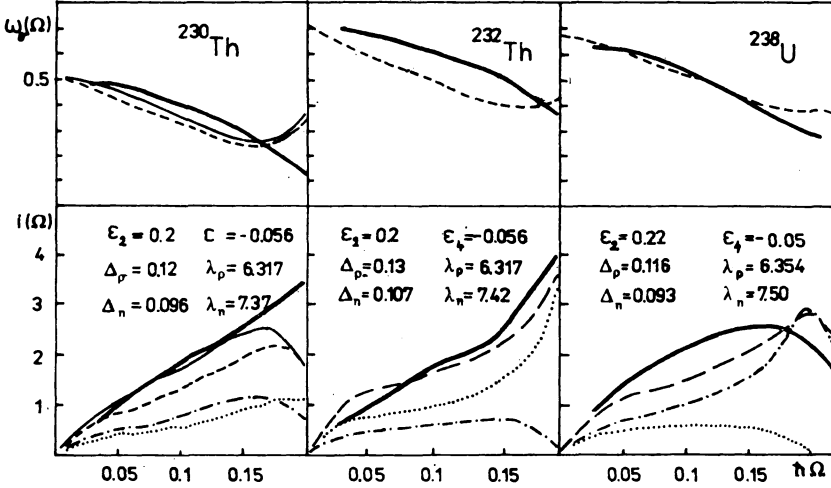


**Fig. 11.** Excitation energy of the vibrational states of the  $K^\pi = 0^-$  band  $\omega_0$  (MeV) and th aligned octupole angular momentum  $i(\Omega)$  as a function of rotational frequencies  $\Omega$  (MeV), (a)  $^{230}\text{Th}$ , (b)  $^{238}\text{U}$ , (c)  $^{232}\text{Th}$ . The solid line corresponds to the experimental values calculated with eq. (65), the thin line to the theoretical calculation for  $\kappa_1/\kappa_0 = 0$  and the dashed line to the case  $\kappa_1/\kappa_0 = -3$ . Proton and neutron contributions are given by the points and point-dashed lines, respectively. The parameters ( $\Delta, \lambda$ ) are given in  $\hbar\omega_0$  units. The experimental data are taken from ref. [39] for  $^{230}\text{Th}$ , ref. [23] for  $^{232}\text{Th}$  and ref. [31] for  $^{238}\text{U}$ .

The isoscalar strength constant  $\kappa_0$  was fixed to reproduce the  $I^\pi = 1^-$  level of the  $K^\pi = 0^-$  band. According to the estimate of ref. [6]  $\kappa_1/\kappa_0 = -3.6$ . The result of calculation for  $\omega_0$  – are not so sensitive to the choice of the ratio  $\kappa_1/\kappa_0$ . We obtain quantitative description of the aligned octupole angular momentum when we take into account only an isoscalar part of the octupole-octupole interaction ( $\kappa_1/\kappa_0 = 0$ ). However, to reproduce simultaneously the alignment and the properties of the electric dipole transition from the octupole states we used the value  $\kappa_1/\kappa_0 = -3$ .

In spite of a very schematic residual interaction in our model, we observed a good agreement of  $\omega_0(\Omega)$  and  $i(\Omega)$  with the experimental data up to 0.17 MeV (see fig. 11). The worse agreement in  $^{230}\text{Th}$  may be due to the Coriolis antipairing effect that decreases the gap at large rotational frequency [6]. Another source of the discrepancy is a possible change in the deformation of the mean field.

Comparing these results with the results of calculations in ref. [26], one concludes that the introduction of effective charges into the octupole operators in the latter paper is not in fact necessary for description of the aligned angular momentum. We obtain the same quality of the description as in ref. [26] for  $^{232}\text{Th}$  in both the cases when  $\kappa_1/\kappa_0 = 0$  and  $-3$ . In  $^{238}\text{U}$  the experimental aligned octupole momentum in the  $K^\pi = 0^-$  band decreases when  $\hbar\Omega \geq 0,16$  MeV (see ref. [31]). We reproduce this tendency in contrast with the results of refs. [21, 26].

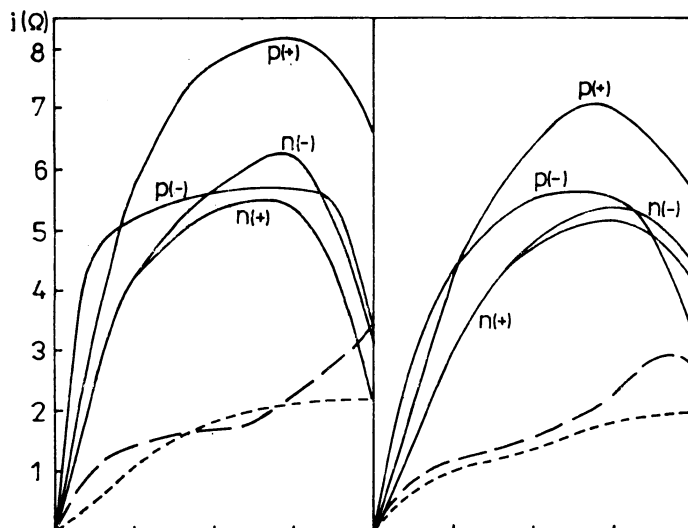


Fig. 12. The aligned angular momentum in the case of (a) uncorrelated pairs corresponding to the lowest negative and positive two-quasiparticle energies (thick line), (b) pure bosons (from ref. [2]) (thin dashed line), (c) our calculation (thick dashed line).

In a pure boson picture [21] (see fig. 12) the aligned vibrational octupole momentum reaches the maximal value  $2-3\hbar$  and remains constant at higher values of the rotational frequency. In this case it is impossible to reproduce the individual character of the alignment because the Coriolis interaction may lead to a constructive or destructive interference of the contributions of different two-quasiparticle components which are absent in a phenomenological picture. On the other hand, the unpaired lower two-quasiparticle components carry a large aligned angular momentum. This is because their structure is defined by the Coriolis mixing of the quasi-protons from  $i_{13/2}$  and  $h_{11/2}$  shells and the quasi-neutrons from the  $j_{13/2}$  and  $i_{13/2}$  shells.

A more sensitive test of the structure of the calculated octupole states is provided by the E1-transitions from these states to the yrast one. Using equations (67) and (68) we calculate the branching ratio  $R_I$  and quantity  $Z$  (see table 5). To describe the experimentally observed ratio  $R_I$ , we have to take into account the isovector part of the octupole-octupole interaction ( $\kappa_0/\kappa_1 = -3$  being the optimal choice).

The semi-microscopic cranking + RPA model allows to describe quite complex mechanism of alignment of octupole vibrational angular momentum in rotational bands  $K^\pi = 0^-$  for  $^{230,232}\text{Th}$ ,  $^{238}\text{U}$  nuclei. Results of calculations demonstrate good agreement with experimental data in values as well as in character of changes of aligned angular momentum and excitation energies caused by octupole correlations in nucleus irrespective of quite simple model residual interactions and using of approximation of fixed model parameters not dependent on rotational frequency.

### 3.3. Giant dipole resonance at high spins

The simple model of Giant dipole resonance was discussed in chapter 2. Here the more realistic approach is used for studying of GDR. At first the average nuclear field is approximated by Nilsson potential. The cranking model calculations based on average field of this type make possible to investigate the evolution of shape of rotating nuclei in broad range of angular momentum [32, 33]. At second, in real experimental conditions the average values of physical quantities are measured which require to use the statistical version of cranking + RPA method. For investigation of energy spectrum of rotating nuclei this version was suggested for the first time in ref. [34]. Besides that the method of strength function (see [1]) was applied for description of electromagnetic transitions from high-excited states.

We restricted ourselves only to dipole-dipole residual interaction so the starting cranking Hamiltonian has the following form

$$(70) \quad H' = \underbrace{\sum_{kl} (\varepsilon_{kl} c_k^+ c_l + \varepsilon_{kl} c_k^+ c_l)}_{H_{AV}(\text{def})} - \Omega I_x - \frac{1}{2} \chi (\hat{\mathcal{D}}_0^{(-)^2} + \hat{\mathcal{D}}_1^{(-)^2} + \hat{\mathcal{D}}_1^{(+)^2}) - \lambda \hat{N}$$

where  $\varepsilon_{kl}$  are the matrix elements of average field potential and other assignment is the same as in [1] and preceding chapters. The symbols  $c_k^+$ ,  $c_k$  represent the creation and annihilation operators of basis single-particle states  $|k\rangle$ ,  $|\bar{k}\rangle$  which are chosen as eigen vectors of the operator  $j_x$ :

$$(71) \quad j_x |k\rangle = m_k |k\rangle, \quad |\bar{k}\rangle = T |k\rangle \quad (|k\rangle = |nljm\rangle)$$

Similarly as in standart version of cranking + RPA method in statistical one in the first step the problem of Hartree is solved. In opposite to normal version in statistical approach the dependence on nuclear temperature (as a measure of average excitation – nuclear heating) is introduced. The problem of Hartree for heated rotating nuclei can be solved for instance by variation method

$$(72) \quad \delta \langle \Omega | H' | \Omega \rangle = 0$$

which gives for single-particle energies  $\xi_k$

$$(73) \quad \xi_k = \frac{\partial \langle \Omega | H_{AV}(\text{def}) - \Omega I_x - \lambda \hat{N} | \Omega \rangle}{\partial \bar{n}_k} = \varepsilon_{kk} - \lambda - \Omega j_{kk}^x$$

where  $\bar{n}_k$  are the occupation numbers depending on nuclear temperature [35]

$$(74) \quad n_k = \langle \Omega | c_k^\dagger c_k | \Omega \rangle = \frac{1}{1 + e^{\xi_k/t}}$$

After the solving of Hartree problem we obtained the average Hartree field in the form

$$(75) \quad H_{HF} = \sum_k (\xi_k c_k^\dagger c_k + \xi_{\bar{k}} c_{\bar{k}}^\dagger c_{\bar{k}})$$

In the following step in analogy with standard version of cranking + RPA method the residual interaction in (70) are involved in the framework of RPA. In statistical version the bosons  $b_{k1}^\dagger$ ,  $b_{\bar{k}1}^\dagger$ ,  $b_{k1}$  (see part 3.1 of this paper and [1]) have two-particle character (in standart version they are represented by two-quasi-particles). Besides that in statistical version we have to use the following commutation relations

$$(76) \quad [c_k^\dagger c_l, c_{k'}^\dagger c_{l'}] \approx \langle \Omega | [c_k^\dagger c_l, c_{k'}^\dagger c_{l'}] | \Omega \rangle = \delta_{kl} \delta_{l'k'} (\bar{n}_k - \bar{n}_l)$$

for determination of energies and structure of phonon describing the coherent excitations of heated system. Otherwise the RPA equation of motion are solved in the same way as in standart version of cranking + RPA (see [1]). Again the Hamiltonian (70) can be divided into the parts with positive and negative signature in consequence of  $R_x(\pi)$  symmetry of average field.

For energy  $\omega$  of phonons with positive signature we obtain the following secular equation

$$(77) \quad \mathcal{F}_{(\omega)}^{(+)} = S^{(+)} + \frac{1}{2\chi} = 0$$

where

$$(78) \quad S^{(+)} = \frac{Z^2}{A^2} S_{1neut}^{(+)} + \frac{N^2}{A^2} S_{1prot}^{(+)}$$

$$S_{1\tau} \equiv \sum_{k>l}^{N_\pi} d_{kl}^{(1+)} \left( \frac{\omega_{kl}(\bar{n}_l - \bar{n}_k)}{\omega_{kl}^2 - \omega^2} + \frac{\omega_{kl}(\bar{n}_l - \bar{n}_k)}{\omega_{\bar{k}l}^2 - \omega^2} \right)$$

$$\omega_{kl} \equiv \xi_k - \xi_l$$

Similarly the secular equation for negative signature phonons has the following form

$$(79) \quad \mathcal{F}^{(-)}(\omega) = \left( S_{00} + \frac{1}{2\chi} \right) \left( S_{11} + \frac{1}{2\chi} \right) - \omega^2 S_{01}^2 = 0$$

where

$$(80) \quad S_{ij} \equiv \frac{Z^2}{A^2} S_{ij}(neut) + \frac{N^2}{A^2} S_{ij}(prot) \quad i, j = 0, 1$$

$$S_{ii}^{(\tau)} \equiv \sum_{kl}^{N_\pi} \frac{\omega_{kl}}{\omega_{kl}^2 - \omega^2} d_{kl}^{(i)} (\bar{n}_l - \bar{n}_k)$$

$$S_{ij}^{(\tau)} \equiv \sum_{kl}^{N\pi} \frac{d_{kl}^{(i)} d_{kl}^{(j)}}{\omega_{kl}^2 - \omega^2} (\bar{n}_i - \bar{n}_k).$$

The symbols  $d_{kl}^{(1+)}$ ,  $d_{kl}^{(i)}$  ( $i = 0, 1$ ) in (78) and (80) represent the particle matrix elements of operators  $\mathcal{D}_1^{(+)}$ ,  $\mathcal{D}_0^{(-)}$ ,  $\mathcal{D}_1^{(-)}$ .

We introduce the partial strength function of reduced probabilities of dipole transitions from one-phonon states to yrast line (see (93) in [1])

$$(81) \quad b(E 1, \tau, \omega) = \sum_i B(E 1, \omega_i^\nu, \tau) \varrho(\omega - \omega_i^\nu)$$

where  $\tau$  is the difference of angular momentum in given transition ( $\tau = 0, 1$ ). The weight function  $\varrho(\omega - \omega_i)$  is given by (91) in [1]. Using the expressions (85) and (86) in [1] for reduced probabilities of dipole transitions and applying the method described in part 2.3.5 of ref. [1] one can obtain the following expressions for partial dipole strength functions:

i) for transition without signature change

$$(82) \quad P_{E1, \tau=0}(\omega) = \frac{1}{\kappa}$$

where the corresponding function  $\mathcal{F}(\omega)$  (see (89) in [1]) is given by (77)

ii) for transitions with signature change

$$(83) \quad P_{E1, \tau=+1}(\omega) = \left[ \frac{2\kappa S_{00} + 1}{2\kappa} \right] \left[ \frac{2\kappa\omega S_{01}}{2\kappa S_{00} + 1} + 1 \right]^2$$

$$P_{E1, \tau=-1}(\omega) = \left[ \frac{2\kappa S_{11} + 1}{2\kappa} \right] \left[ \frac{2\kappa\omega S_{01}}{2\kappa S_{11} + 1} + 1 \right]^2$$

with corresponding function  $\mathcal{F}(\omega) = \mathcal{F}^{(-)}(\omega)$  given by (79).

The single-particle energies in rotating system were obtained by diagonalization of Nilsson Hamiltonian with cranking term. The equilibrium deformation parameters ( $\varepsilon, \gamma$ ) were determined by searching of minimum of thermodynamic potential (that means for given temperature  $t$  and rotational frequency  $\Omega$  (see [32] and [33]). Strength constant  $\kappa$  in residual interaction was chosen so in order to reproduce the position of GDR in spectrum (that means according to expression  $\kappa = 1200 \text{ A}^{-5/3} \text{ MeV/fm}^2$ ). The width  $\Delta$  for averaging of strength function (see (91) in [1]) is  $\Delta = 1.5 \text{ MeV}$ .

The dependence of partial strength functions of isovector dipole excitations in dependence on angular frequency is shown in fig. 13 for  $^{160}\text{Yb}$  nucleus in  $t = 0 \text{ MeV}$ . In deformed nucleus with axial symmetry (which occurs for  $\Omega = 0$ ) the dipole resonance is splitted into two components. With increasing angular frequency when nuclei acquires the nonaxial deformation characterised by parameter  $\gamma$  there are three components in structure of GDR which correspond to  $\tau = 0, +1$ .

In fig. 14 the total strength functions of  $^{152}\text{Sm}$ ,  $^{160}\text{Yb}$  and  $^{180}\text{Os}$  are shown in dependence on angular frequency  $\Omega$ . The shape of  $^{152}\text{Sm}$  and  $^{160}\text{Yb}$  changes with



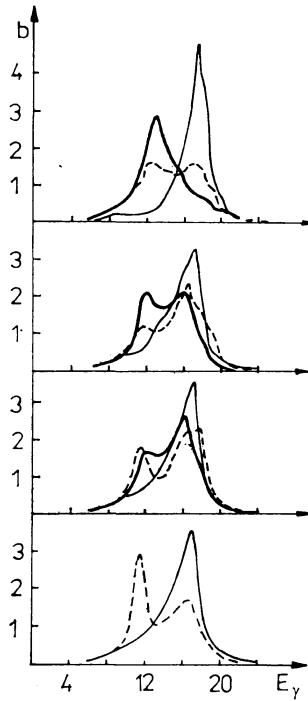


*Fig. 13.* Partial strength functions of isovector dipole excitations for  $^{160}\text{Yb}$  for different values of rotational frequencies  $\Omega$ . In the left side of each figure the conditions of calculation are given and in the right side there are values of strength function in oscillator case and corresponding position of oscillator frequency is shown by arrows in energy axis. The thin line corresponds to the strength function  $b_{\tau=0}$ , thick one to  $b_{\tau=+}$  and pointed to  $b_{\tau=-}$ .

increasing  $\Omega$  approximately in the same manner while  $^{180}\text{Os}$  acquires the quite high nonaxiality as a result of rotation. Such dependence of shape on rotation is reflected also in character of strength functions. Similar behaviour of strength function in dependence on energies of  $\gamma$ -quanta for different values of  $\Omega$  can be seen for  $^{160}\text{Yb}$  and  $^{152}\text{Sm}$ . Probably the predominant neutron number in  $^{152}\text{Sm}$  ( $N = 90$ ) as well as in  $^{160}\text{Yb}$  ( $N = 90$ ) determines the behaviour of strength function in rotation. The character of changes of strength function of  $^{180}\text{Os}$  in dependence on energy of  $\gamma$ -quanta in sufficiently high rotational frequency differ considerably from the behaviour of strength function of  $^{152}\text{Sm}$  and  $^{160}\text{Yb}$ . This part is probably caused by different ability for deformation for  $^{152}\text{Sm}$  and  $^{160}\text{Yb}$  in comparison with  $^{180}\text{Os}$ . The bigger ability for deformation the higher splitting of components of isovector dipole resonance can be observed and consequently the broader region of localisation of GDR is found. That means that in fast rotation when large deformation occurs the region of localization of GDR must be broader than in the case of low angular momenta.

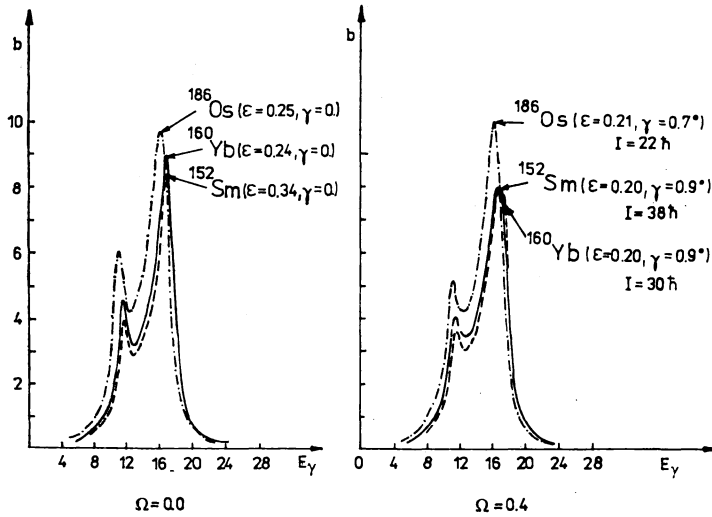


**Fig. 14.** Total strength functions for nuclei  $^{152}\text{Sm}$ ,  $^{160}\text{Yb}$  and  $^{180}\text{Os}$  at different values of rotational frequencies  $\Omega$ . In brackets the equilibrium deformation parameters and the values of angular momentum  $I$  (corresponding to given maximal value of  $\Omega$ ) are shown [33].

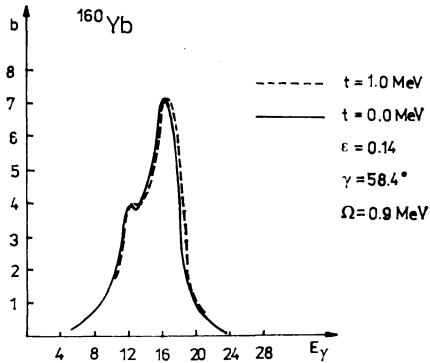


**Fig. 15.** Total strength functions of isovector dipole excitations in  $^{160}\text{Yb}$  for different temperatures.

The total strength functions of  $^{160}\text{Yb}$  for  $t = 0$  and 1 MeV are demonstrated in fig. 15. The deformation parameters for  $t \neq 0$  case are taken from ref. [33]. The heating of nuclei in rotating case in comparison with nonrotating one doesn't influence considerably GDR (see [36]). In this sense it is necessary to note that in obtaining of fig. 15 the deformation of average field has been independent on nuclear temperature. In fact the temperature effects substantially influence the nuclear shape (see [33]) and therefore one can expect that character of strength function of GDR is dependent on temperature through the change of average field.

#### 4. Conclusion

The investigation of high excited and high spin states represents the new quickly developing region of low energy nuclear physics. The studying of nuclei by means of new nonstandart experimental method stimulated the progress of new theoretical approaches. One of these approaches is represented by cranking + RPA method. The further development of this method is connected with the determination of symmetries which are conserved in nuclear rotation when strong Coriolis interaction doesn't allow to classify the nuclear levels by means of the projection  $K$  of angular momentum onto symmetry axis. Conservation of nuclear symmetry with respect to rotational axis lead to introduction of new quantum number – signature. This quantum number makes possible to understand a lot of regularities in experimental data on rotating nuclei [37, 38]. The possibility of classification of the states according to signature unable also to solve the serious technical problems in solving the Hartree-Fock-Bogolubov equations in cranking model.

The cranking + RPA method described in [1] and in this paper allow to investigate qualitatively and quantitatively the collective as well as noncollective states in broad region of angular momentum and excitation energy. In spite of the fact that this method was firstly suggested for investigation of high-spin states its applicability for description of low-lying states gives evidence for its universal use. Nevertheless for obtaining of more detailed information on transition character it is necessary to go beyond the framework of RPA and to involve into Hamiltonian and into transition operators the terms of higher order of boson expansions of single-particle operators. The importance of such effects can be expected in the first place for description of low-spin region of spectrum because the signature is a good quantum number only for sufficiently high rotational frequency  $\Omega$ . The quality of calculation in the framework of cranking + RPA method can be also improved by means of taking into account of residual interactions which correspond to precise restoration of translational and rotational symmetries of Hamiltonian violated by deformed nuclear average field.

#### References

- [1] KVASIL J., NAZMITDINOV R. G., Acta Universitatis Carolinae, Math. Phys. 29 (1988), 30.
- [2] RIPKA G., BLAIZOT J. B., KASSIS N., Heavy Ions High Spin States and Nuclear Structure, IAEA Vienna, Vol. 1 (1975), 445.
- [3] ZELEVINSKIJ V. G., Yad. Fizika 22 (1975), 1085.
- [4] AKBAROV A., et al., JINR Communication P4-12772, Dubna 1979.
- [5] AKBAROV A., et al., Yad. Fizika 33 (1981), 1480.
- [6] BOHR A., MOTTELSON B., Nuclear Structure, Vol. II, Benjamin N. Y. 1974.
- [7] COHEN S., PLASIL F., SWIATECKI W. J., Ann. Phys. 82 (1974), 557.
- [8] MIKHAILOV I. N., BALBUTSEV E. B., BRIANCON CH., Nuclear Collective Dynamics Poiana Brasov, Romania, 1982, p. 263.
- [9] IGNATYUK A. V., MIKHAILOV I. N., Yad. Fizika 33 (1981) 919.

- [10] PYATOV N. I., Materials of XI winter school LINP, part 1 (1976) 156.
- [11] SOLOVIEV V. G., Theory of Complex Nuclei, NAUKA, Moskva 1971.
- [12] DUDEK J., et al., J. Phys. G5 (1979) 1259.
- [13] DUDEK J., WERNER T., J. Phys. G4 (1978) 1543.
- [14] STRUTINSKY V. M., Nucl. Phys. A 122 (1968) 1.
- [15] CWIOK S., et al., Proc. of XVI Winter School Bielsko-Bialo, Poland 1978, Vol. 2, p. 588.
- [16] KVASIL J., et al., Izv. USSR, ser. fiz. 48 (1984) 844.
- [17] GRIGORIEV E. P., SOLOVIEV V. G., Structure of Even Deformed Nuclei, NAUKA, Moskva 1974 (in russian).
- [18] BOHR A., MOTTELSON B., Phys. Scripta 25 (1982) 28.
- [19] DUMITRESCU T. S., HAMAMOTO I., Nucl. Phys. A301 (1982) 263.
- [20] MIKHAILOV I. N., USMANOV P. N., CHARIEV M. M., JINR preprint P4-84-475 Dubna 1984.
- [21] MIKHAILOV I. N., et al., Yad. Fizika 38 (1983) 297.
- [22] BRIANCON CH., MIKHAILOV I. N., Proc. Int. School in Nucl. Structure Alushta, Oct. 1985 eds. V. G. Soloviev and Yu. P. Popov, D4-85-851, p. 245.
- [23] BRIANCON CH., MIKHAILOV I. N., Sov. J. Part. Nucl. 13 (1982) 101.
- [24] NAZMITDINOV R. G., FRAUENDORF S., Yadernaya spektroskopiya i struktura atomnovo yadra, Tesisy dokladov XXXV soveschaniya (Leningrad 1955) (Nauka Moskva) p. 166 (in Russian).
- [25] NAZMITDINOV R. G., MIKHAILOV I. N., BRIANCON Ch. Phys. Lett. B 188 (1987) 171.
- [26] ROBLEDO L. M., EGIDO J. L., RING P., Nucl. Phys. A449 (1986) 201.
- [27] KOCHBACH L., VOGEL P., Phys. Lett. B32 (1970) 434.
- [28] CHEN Y. S., FRAUENDORF S., Nucl. Phys. A393 (1983) 135.
- [29] FRAUENDORF S., SIMON R. S., preprint GSI 80-25 (1980).
- [30] EGIDO J. L., RING P., Nucl. Phys. A423 (1984) 93.
- [31] GROOSE E., et al.: Phys. Rev. Lett 35 (1975) 565, Phys. Scr. 24 (1981) 337.
- [32] IGNATYUK A. V., et al., Phys. Lett. B76 (1978) 543.
- [33] IGNATYUK A. V., et al., Nucl. Phys. A364 (1980) 191.
- [34] IGNATYUK A. V., MIKHAILOV I. N., Yad. Fizika 30 (1979) 665.
- [35] IGNATYUK A. V., Yad. Fizika 17 (1973) 502.
- [36] BAZNAT M. I., IGNATYUK A. V., PYATOV N. Y., Yad. Fizika 30 (1979) 949.
- [37] BENGTSOON R., FRAUENDORF S., Nucl. Phys. A327 (1979) 139.
- [38] RAGNARSSON I., ABERG S., SHELINE R. K., Phys. Scr. 24 (1981) 215.
- [39] GERL J., et al., Phys. Rev. C24 (1984) 1684.